University of Twente

Bachelor thesis

1D numerical analysis of heat transfer in supercritical water in a heated tube and a single shell and tube heat exchanger

Author:
T.P. van der Wel

Supervisors:
S.O. Odu
Dr. Ir. A.G.J. van der Ham
Prof. Dr. H.J.M. Bouwmeester

22/06/2015

1 Abstract

Supercritical water has found many applications in the last decade and the range of applications keeps growing with time. These applications , such as the desalination of sea water and the gasification of biomass are based on the tunability of the properties of supercritical water. The energy requirement of these processes at supercritical conditions can be a draw back in the commercial scale-up. The energy necessary to bring water from standard ambient conditions to supercritical conditions of 300 bar and 450 °C is 3 $\frac{MJ}{kg}$ [1]. A heat exchange apparatus is installed to use the heat of the product stream for the feed stream. To optimize the heat exchange apparatus a 1D model is developed to numerically calculate the heat exchange inside a heated tube and a single tube and shell heat exchanger. Both the models are executed in Matlab and validated through experimental data. The calculated values from the heated tube simulation are in agreement with the experimentally obtained data. The calculated values from the heat exchanger are not in agreement with the experimental data. The Nusselt correlations used in the heat exchanger simulation is not valid for the experimental conditions.

Contents

2 Introduction

The properties of water at supercritical conditions are researched and applied in various chemical processes. Water becomes supercritical at (P >221.2 bar, T >374.15 °C) [2]. The physical properties of water drastically change at the critical point [3]. There is no phase transition present. The single liguid phase can behave like liquid or vapor when the properties are tuned. The density for instance decreases vastly, while the heat transfer coefficient increases rapidly.

The solvation behaviour of supercritical water is used in the desalination process of sea water. At supercritical conditions the solubility of the salt goes close to zero and can be easily filtered away. This leaves only a clean water stream without any liquid waste streams.[4]

Another process is the reaction of supercritical water with wet biomass streams. The supercritical water reacts with the biomass to form a gas, rich of methane and hydrogen. The wet biomass therefore does not have to be dried before further processing is possible.[5]

Water at supercritical conditions offers the ability to tune properties for these and other processes. The tuning of properties and the operating of the processes at supercritical conditions requires a large energy consumption. To make the process commercial viable the energy costs need to be reduced. Energy consumption can be greatly reduced by heat integration. This is achieved by placing a heat exchanger between the supercritical product stream and the feed stream.[6]

This report focusses on the numerical analyses of heating water at sub and supercritical conditions inside a tube heated by heating elements on the wall and the numerical analyses of the heat exchange between two water streams in a single shell and tube. The models are developed in Matlab.

Both models are based on the Nusselt correlation with a mass flux below 20 $\frac{kg}{m^2 s}$. The correlations were obtained from previous research[7]. Lab scale set ups are frequently operated at lower mass fluxes. The numerical analysis of a lab scale heat exchange can give insight in the set up. The simulation is done in the 1 dimensional axial direction. This is more approriate in the engineering design of a heat exchange apparatus. Literature does not discuss the modeling of heat exchange with a low mass flux. The low flux ensures the natural convection is critical in the heat exchange. In literature there are already Nusselt correlations present for mass fluxes above 200 $\frac{kg}{m^2 s}$ [8] [9]. The high mass flux ensures the major heat exchange occurs by forced convection. In commercially scaled heat exchangers a large mass flux is common. No further research is done for heat exchange systems with non-negligible natural convection.

3 Model information

Both the temperature profiles of a heated tube and a heat exchanger are evaluated in Matlab. Matlab is a well suited program to develop a 1 dimensional model. The validation of the models is done with both experimental results and with Comsol calculations [7]. The mass flux is kept low during the process. This is to ensure natural convection is important. Natural convection is induced by a temperature difference inside the fluid. The temperature difference allows for natural transfer of heat. The forced convection is due to the fluid velocity. The velocity of the fluid is kept low for natural convection to not be negligible.

This report states the development of two 1 dimensional Matlab models for a heated tube and heat exchanger at supercritical conditions with a low mass flux. A 2 dimensional heat exchanger model is already present in literature, developed in Comsol [7]. The Comsol model is validated by experiments. The Nusselt correlations are obtained by the 2D Comsol model, but are also validated in the 1D direction. The 1D Nusselt correlations are used to develop the Matlab model. The 2 dimensional model is complicated and takes a lot of time to simulate. A 1 dimensional model is developed because of the shorter simulation time and it is also more appropiate in engineering designs and optimizations. The Matlab models give a quick prediction about designing parameters of the heated tube and the heat exchanger, but can also be used to estimate energy efficiencies without running expensive and time consuming experiments.

The models are developed in Matlab and validated by experimental and Comsol data. The heated tube is validated by values from the Comsol model [7], previous research data [10] and newly done experiments on the set up. Previous experimental data only measure the tube stream temperature, but does not measure the inner wall temperature. The heat exchanger is only validated with experimental data obtained from the prototype heat exchanger.

The Nusselt correlations [7] used in the models are valid for mass fluxes below the 20 $\frac{kg}{m^2 s}$ where natural convection is important. The correlations are based on a laminar flow profile in a vertical tube. The developed Matlab models can therefore be used for processes within these conditions.

3.1 Fluid dynamics

The Reynolds number gives an indication about the type of flow that is present. A Reynolds number (equation (1)) below 2300 indicates that the flow is in the laminar regime and above 4000 in the turbulent regime. The region between 2300 and 4000 is a transition area [11, ch.5]. The calculations for the Reynolds number were performed with Matlab using XSteam [1].

$$Re = \frac{G * d}{\eta} \tag{1}$$

The Reynolds number indicates the flow regime that is present due to the forced convection. The low mass flux ensures that free convection also plays a major part in the heat transfer. The free convection is induced by the temperature difference of the inner wall and the bulk of the fluid. The temperature difference also has an influence on the density of the fluid. The physical properties, like the density, vary drastically with only a small temperature change [12]. The density difference improves the magnitude of the free convection.

The radial temperature profile is averaged over the radial positions by introducing the mixing cup temperature. The mixing cup temperature is the average temperature measured when the fluid is collected and mixed in a cup [13, ch.3]. The definition of the mixing cup temperature is stated in equation (2).

$$T_{mc} = \frac{\int_0^{r_t} G(r,z) C_p(r,z) T(r,z) 2\pi r dr}{\int_0^{r_t} G(r,z) C_p(r,z) 2\pi r dr} \tag{2}$$

The type of heat transfer inside the stream is calculated with the Rayleigh number (equation (3)). The Rayleigh number indicates if the heat is transferred mainly by conduction or convection. The Rayleigh number is dependent on the Grashof number (equation (4)) and the Prandtl number (equation (6)). The Grashof number gives an indication about the order of magnitude of natural convection.

The Reynolds number gives an indication about the flow regime, if the stream is laminar or turbulent. The Grashof number states the order of magnitude of natural convection. This indicates the importance of natural convection for the heat exchange inside the stream.

$$Ra = GrPr = \frac{g d^3 \rho^2 C_p \beta}{\eta k}(T_w - T_{mc}) \tag{3}$$

$$Gr = \frac{g d^3 \beta \rho^2}{\eta^2}(T_w - T_{mc}) \tag{4}$$

$$\beta = \frac{1}{\rho}(\frac{\delta\rho}{\delta T} \tag{5}$$

$$Pr = \frac{\eta C_p}{k_{wa}} \tag{6}$$

3.2 Nusselt correlation

The heat transfer coefficient inside the shell and tube vary along the axial direction. The physical properties are dependent on the fluid and the fluid properties are dependent on temperature. The heat transfer in the heated tube and single shell and tube are determined by both forced and free convection. The heat transfer coefficient of the process is dependent on both types of convection. The 1 dimensional Nusselt correlation for the heat transfer coefficient inside the tube is shown in equation (7) and the Nusselt correlation for the heat transfer coefficient on the shell side is shown in equation 8. The Nusselt correlations are determined based on a 2D Comsol model and validated for the 1 dimensional model [7]. The Nusselt correlations for both the shell and tube are valid at the conditions of table 1. The Comsol values which were used to validate the correlation where obtained from a vertical single shell and tube heat exchanger[7].

$$Nu_t = \frac{hd_t}{k_{wa}} = 0.91 Gr^{0.3} Re^{-0.2} (\frac{C_{p,w}}{C_{p,mc}})^{0.3} \tag{7}$$

$$Nu_s = \frac{hd_h}{k_{wa}} = 0.42 Gr^{0.4} Re^{-0.3} (\frac{C_{p,w}}{C_{p,mc}})^{0.4} \tag{8}$$

Table 1: Boundary conditions for the Nusselt validation [7]

	Tube	Shell
Mass flux	7, 20 $[\frac{kg}{m^2 s}]$	1.3, 7$[\frac{kg}{m^2 s}]$
Diameter	$d_t = 1$ cm	$d_h = 0.36$ cm
Reynolds	1000-6500	50 - 725
Pressure	300 bar	300 bar

The Nusselt number is dependent of the Reynolds number (equation (1)) and the Grashof number (equation (4)). The hydraulic diameter (equation (9)) is used to calculate the shell side heat transfer coefficient. The tube is stationed inside the shell, the effective shell side diameter is therefore calculated with the hydraulic diameter.

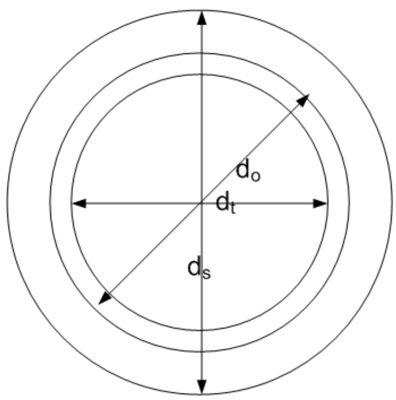

Figure 1: Hydraulic diameter

$$d_h = 4\frac{\frac{1}{4}\pi(d_s^2 - d_o^2)}{\pi(d_s - d_o)} = d_s - d_o \tag{9}$$

4 Heated tube model

The heated tube is used in the process to pre-heat the feed stream. The heated tube model is used to gather information about the heat transfer inside the tube and the temperature profile of the water inside the tube. The model can help optimize the heating process without running expensive and time consuming experiments. A simplified drawing of the heated tube is shown in figure 2. The tube is divided into a number of small sections.

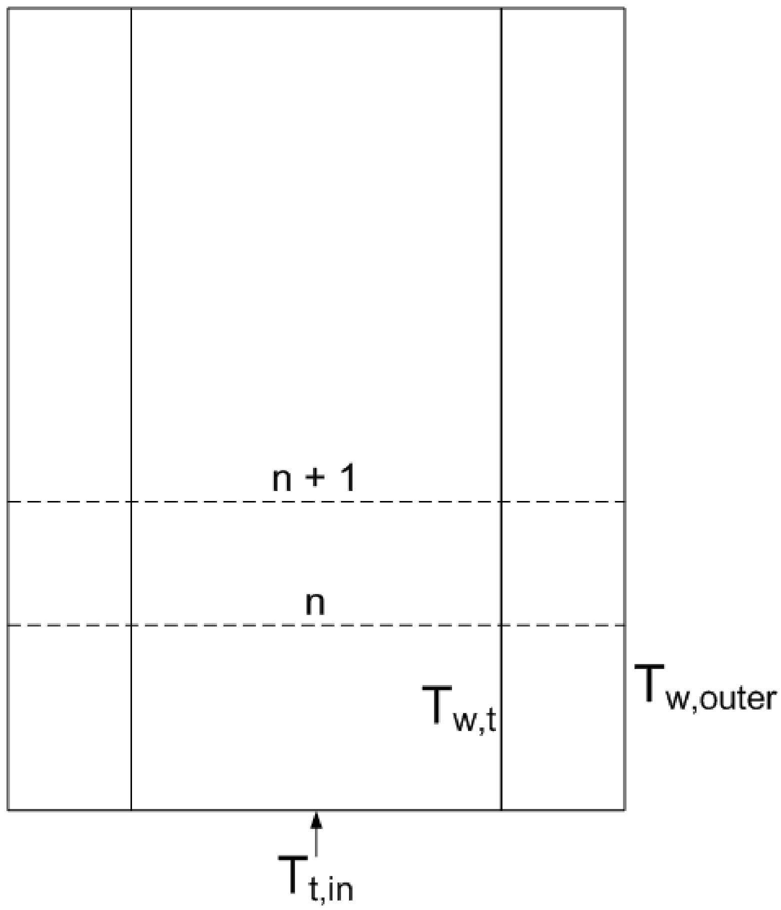

Figure 2: Schematic figure of the heated tube

In order to develop the model a heat balance is necessary to incorporate the heating of the tube stream via the wall. Each heating block is set to a certain temperature, but due to the tube stream a temperature gradient exists along the axial direction.

4.1 Heat balance

It is assumed that there are no heat losses to the environment, because of the insulation. The law of energy conservation is applied inside the tube (equation (10)). The inlet conditions: inlet tube stream temperature, pressure, outer wall temperature profile, mass flow, are constants and can be set to a fixed value before the simulation. The tube is divided into a small number of sections over which the equation (10) is calculated. The heat balance reached stationary conditions.

$$Q_{out} = Q_{in} + Q_{wall} \tag{10}$$

The heat transfer from the wall is obtained with equation (11).

$$Q_{wall} = UA_t(T_{w,outer} - T_{mc,t}) \tag{11}$$

$$\frac{1}{U_t} = \frac{r_t ln(r_o/r_t)}{k_s} + \frac{1}{h_t} \tag{12}$$

$$Q_{in} = \phi_m H(p, T) \tag{13}$$

The heat balance is developed for a 1 dimensional heated tube. Only the axial temperature profile is obtained. The inner wall temperature of the heated tube is calculated by the heat balance for the wall heat flow, equation (14).

$$Q_{wall} = \frac{2\pi dz k_{st}}{\ln(\frac{r_o}{r_t})}(T_{w,outer} - T_{wall,t}) \tag{14}$$

4.2 Assumptions

The heat losses are assumed to be negligible. All the heat that is transferred from the heating blocks on the wall is used to heat up the fluid inside the tube. The only heat flow that enters the tube is via the wall.

The conductive heat flow through the wall is dependent on the tube side inner wall temperature and the outer wall temperature fixed by the heating blocks. This temperature difference ensures the heat flow. At an increasing tube side inner wall temperature the heat flow gradually decreases until the tube temperature becomes stable and there is no more heat transfer.

The tube is divided into a fixed number of sections. The calculation are based on an iteration method, giving an approximation of the differential heat equation. Increasing the number of sections ensures a better model prediction, but increases the time it takes to simulate. A tolerance factor is used to compare the guessed overall heat transfer coefficient with the calculated value. The magnitude of this tolerance increases the precision of the model, but is also important in the required simulation time.

The thermal conductivity [10] of the stainless steel wall is temperature dependent, appendix (chapter 16). In the model the conductivity is calculated with the mean wall temperature. Due to the fact that the wall is thin the temperature profile inside the wall is assumed to be linear. The thermal conductivity in the model can be slightly different then it is in practice.

The pressure drop is relatively small at the operating pressure around 300 bar. The difference between the in and outlet pressure is less then 1 bar. This small difference is neglected in the developed heated tube model.

The outer wall temperature measured experimentally is the input for the calculations of the validation cases. The wall temperature is measured at several axial positions. The outer wall temperature is made continuous by linear interpolation between the data points. The interpolation method gives the best approximation of the outer wall profile, because of the irregular shape. The amount of data points and therefore the accuracy of the outer wall profile indicate the precision of the predicted tube stream temperature and inner wall temperature profiles.

The fouling inside the tube is assumed to be negligible. The fouling constant is therefore neglected from the overall heat transfer coefficient.

4.3 Model

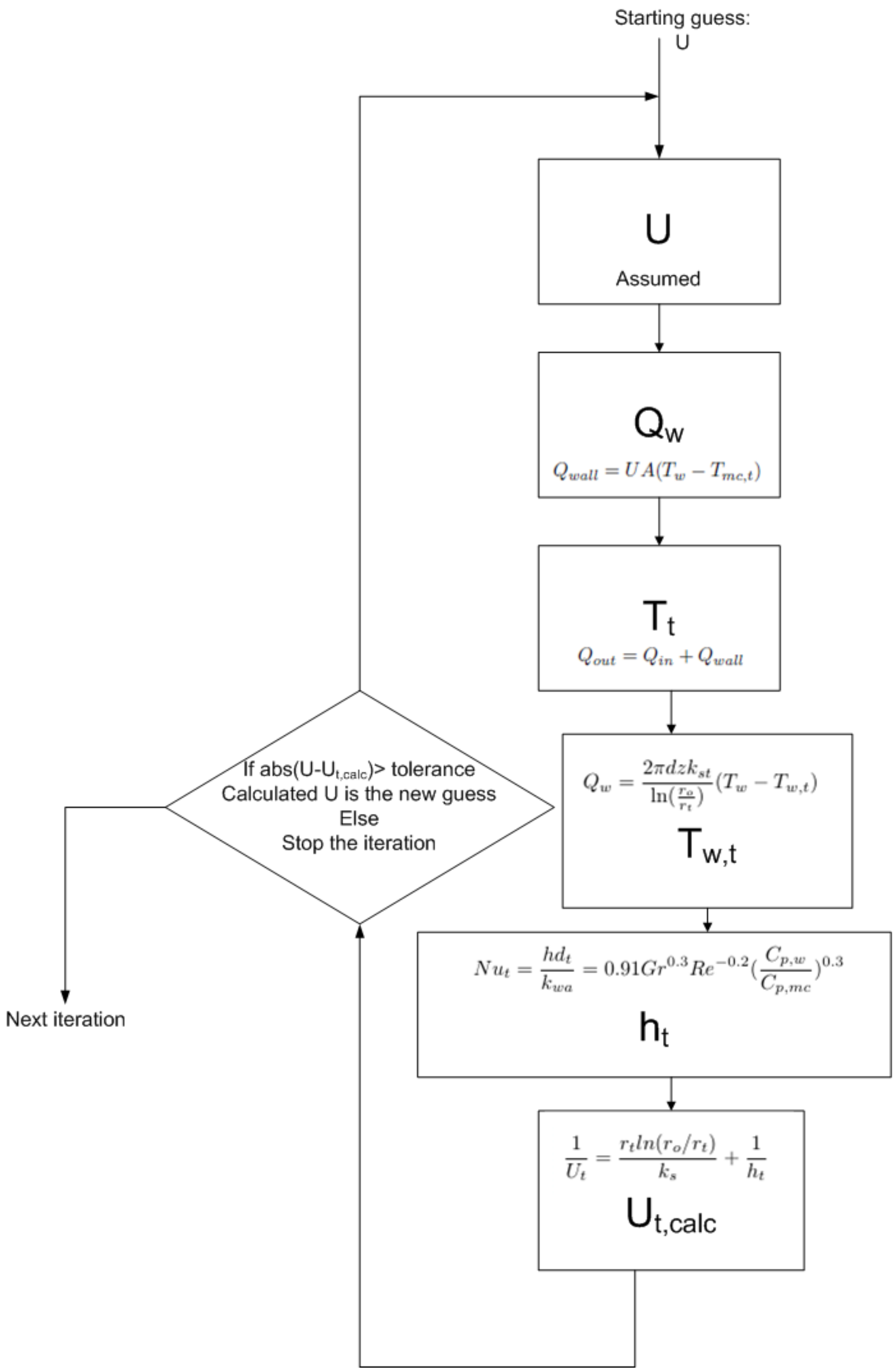

Figure 3: Graphic scheme heated tube per section

The heated tube model is developed for a single heated tube. The outer wall temperature is fixed by the heating elements. With the balance of equation (10) the temperature profile inside the tube is determined through iterations. The model is based on the iteration of a fixed number of sections. The overall heat transfer coefficient is assumed and the height of each section is fixed to a constant value. With the assumed overall heat transfer coefficient, the temperature inside the bulk of the section is calculated. Next the heat flow in each section, the tube side inner wall temperature, the heat transfer coefficient and finally the overall heat transfer coefficient. The calculated overall heat transfer coefficient,(12) , is compared with the assumed value. The calculations are iterated until the calculated value matches the assumed value. The systematic iteration of each axial section is shown in figure 3. The inlet conditions are also the starting positions of the iterations. The length of the overall heated tube is fixed. Calculations are continued for each section until the total number of sections is obtained. The outlet temperature of each section is calculated with the heat flow from the wall. The average bulk temperature of each section is estimated with the logaritmic mean temperature (equation (24)).

$$T_{lm,t} = \frac{T_{t,n+1} - T_{t,n}}{\ln \frac{T_{t,n+1}}{T_{t,n}}} \tag{15}$$

5 Heat exchanger model

The developed model for the single shell and tube heat exchanger helps optimize the heat transfer between the shell and tube streams. The process consists of a counter current single shell and tube heat exchanger. The simplified heat exchanger is shown in figure 4.

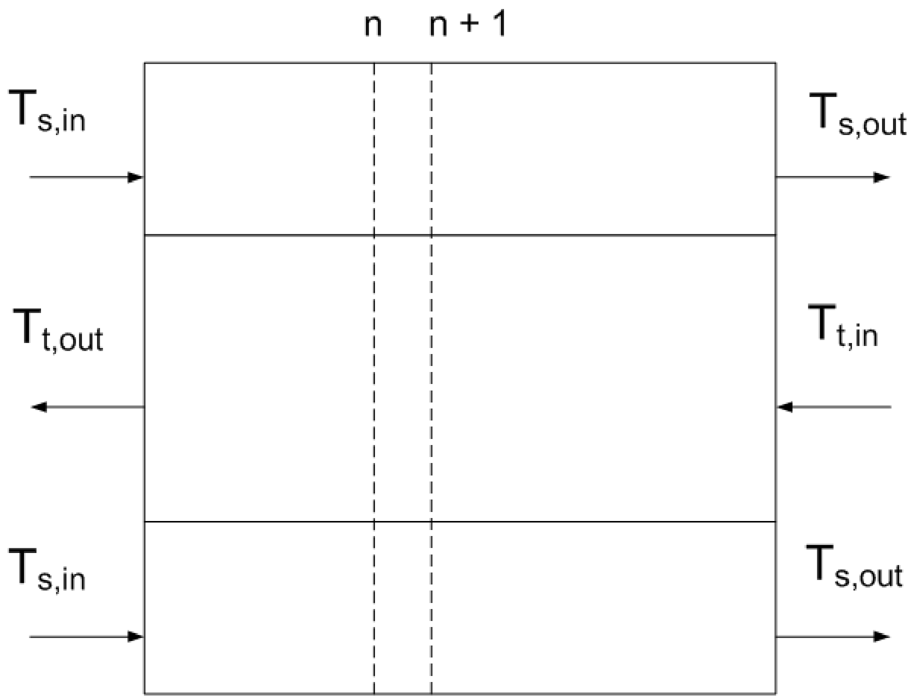

Figure 4: Simplifed heat exchanger

There are two shell and tube configuration that are used in the development. The first is where the hot stream enters the tube and the cold stream enters the shell. The second configuration is where the hot stream enters the shell and the cold stream enters the tube. For both configurations a Matlab model is developed. The theory is explained through the hot shell and cold tube set up, but both configurations are explained in section 5.5.

5.1 Heat balance

The heat exchanger model is derived from the heat balance for the second configuration. The temperature in the cold tube stream will increase, while the temperature of the product stream in the hot shell stream decreases. For the shell side of the heat exchanger the heat balance is derived in respectivelly equation (16) and equation (17). It is assumed that the heat flow from the shell side stream is equal to the heat flow to the tube side stream. The axial position is fixed in the derivation. The counter-current heat exchange calculations are based on figure 4. Although the fluids move in the opposite direction. The calculations are started from the same axial point. The outlet temperature of the shell fluid and the inlet temperature of the tube fluid are the starting point. Both the shell and tube side fluids increase in temperature due to the same axial starting position.

$$0 = \phi_{m,s} C_p T_z - \phi_{m,s} C_p T_{z+dz} - h_s \pi d_o dz (T_{w,s} - T_{mc,s}) \tag{16}$$

$$\frac{T_{z+dz} - T_z}{dz} = \frac{-h_s \pi d_o}{\phi_{m,s} C_p} (T_{w,s} - T_{mc,s}) \tag{17}$$

The heat balance for the tube is comparable with the shell. The derivation of the heat balance is done with equation (18) and (19).

$$0 = \phi_{m,s} C_p T_z - \phi_{m,t} C_p T_{z+dz} - h_t \pi d_t dz (T_{w,t} - T_{mc,t}) \tag{18}$$

$$\frac{T_{z+dz} - T_z}{dz} = \frac{h_t \pi d_t}{\phi_{m,t} C_p} (T_{w,t} - T_{mc,t}) \tag{19}$$

5.2 Shell and Tube temperature

The inlet shell and tube side temperatures are fixed. The amount of heat that can be transferred through the wall for every section is calculated with equation (20).

$$Q_{wall} = U_{hex,o} A_o (T_{mc,s} - T_{mc,t}) \tag{20}$$

$$\frac{1}{U_{hex,o}} = \frac{1}{h_s} + \frac{d_o \ln \frac{r_o}{r_i}}{2k_t i} + \frac{1}{h_t}\frac{d_o}{d_t} \tag{21}$$

The shell stream temperature will decrease, because it releases heat to the fluid tube stream. The overall heat transfer coefficient based on the outer tube diameter (equation (21)) [14] is dependent on the heat transport coefficient of both the shell and tube stream, but also on the thickness and the type of the wall.

The calculated overall heat transfer coefficient (equation (21)) is used to predict the heat transfer from the wall. The relation for the heat flow from the wall is stated in equation (20). The logaritmic mean temperature is used to calculated the average temperature per section.

The heat exchanger is divided into small axial length sections. The sections are used to iteratively simulate the heat exchanger. The length of the heat exchanger is fixed. The number of steps in the axial direction determines the precision of the calculations. The heat transfer inside each section is calculated with a heat balance (equation (22). The heat flow is stated as the heat flow directed from the wall. The complete heat flow is from the hot shell side stream to the colder tube side stream. The wall abbreviation is used, because the heat flow through the wall is the same as the total heat flow.

$$H_{n+1}\phi_m = H_n \phi_m + Q_{w,n} \tag{22}$$

The heat flow from each wall section varies for different axial positions. The length of each section is assumed to be equal. The length, mass flow, pressure, the inlet temperature of the tube side and the inlet temperature of the shell side are fixed. With XSteam [1] the enthalpy at the inlet of the first section can be calculated and therefore the temperature at the outlet of the first section. Iterations give the temperature profile inside the shell and the tube. These temperatures are used to calculated the mean temperatures per section. The physical properties differ with temperature. The average temperature is used to calculated the average value of the physical properties per section. The average temperature of the shell and tube per section are respectively shown in equation (23) and (24). The average temperatures in the shell and in the tube are assumed to be equal to the mixing cup temperatures, equation 2, that would be present.

$$T_{lm,s} = \frac{T_{s,n+1} - T_{s,n}}{\ln \frac{T_{s,n+1}}{T_{s,n}}} \tag{23}$$

$$T_{lm,t} = \frac{T_{t,n+1} - T_{t,n}}{\ln \frac{T_{t,n+1}}{T_{t,n}}} \tag{24}$$

5.3 Wall temperatures

The Titanium wall that seperate the shell fluid and tube fluid is important in the heat transfer determination. The temperature on the hot shell side of the wall is higher then the temperature on the cold tube side of the wall. With both balances of equation (17) and (19) the wall temperature of both sides can be calculated. The rewritten equations are depicted in equation (25) and (26).

$$T_{w,s} = T_{mc,s} - \frac{\phi_{m,s} C_p}{h_s \pi d_o} \frac{T_{z+dz} - T_z}{dz} \tag{25}$$

$$T_{w,t} = T_{mc,t} + \frac{\phi_{m,t} C_p}{h_t \pi d_t} \frac{T_{z+dz} - T_z}{dz} \tag{26}$$

The wall thickness is thin and therefore the temperature profile inside the wall is assumed to be linear. The average wall temperature is calculated with equation (27).

$$T_{w,av} = \frac{T_{w,s} + T_{w,t}}{2} \tag{27}$$

5.4 Assumptions

The heat exchanger is divided into a fixed number of sections. Each section has the same area and axial length. The sections are used in the iterations.

The wall thickness is assumed to be thin. The temperature profile inside the wall is therefore assumed to be linear. The thermal conductivity of the titanium wall is temperature dependent, appendix (chapter 16). The thermal conductivity[15] in the wall is calculated with the average wall temperature .

The pressure drop inside the tube and shell streams are assumed to be negligible.

The averages temperature inside each section is calculated with the logaritmic mean temperature definition. The average temperature offers a prediction for the mixing cup temperature that is present in practice and is used to calculate the values of the different physical properties necessary with XSteam [1].

The fouling of the tube and shell due to the continuous water flow is neglected. The overall heat transfer coefficient therefore does not contain the fouling constants of water.

5.5 Model

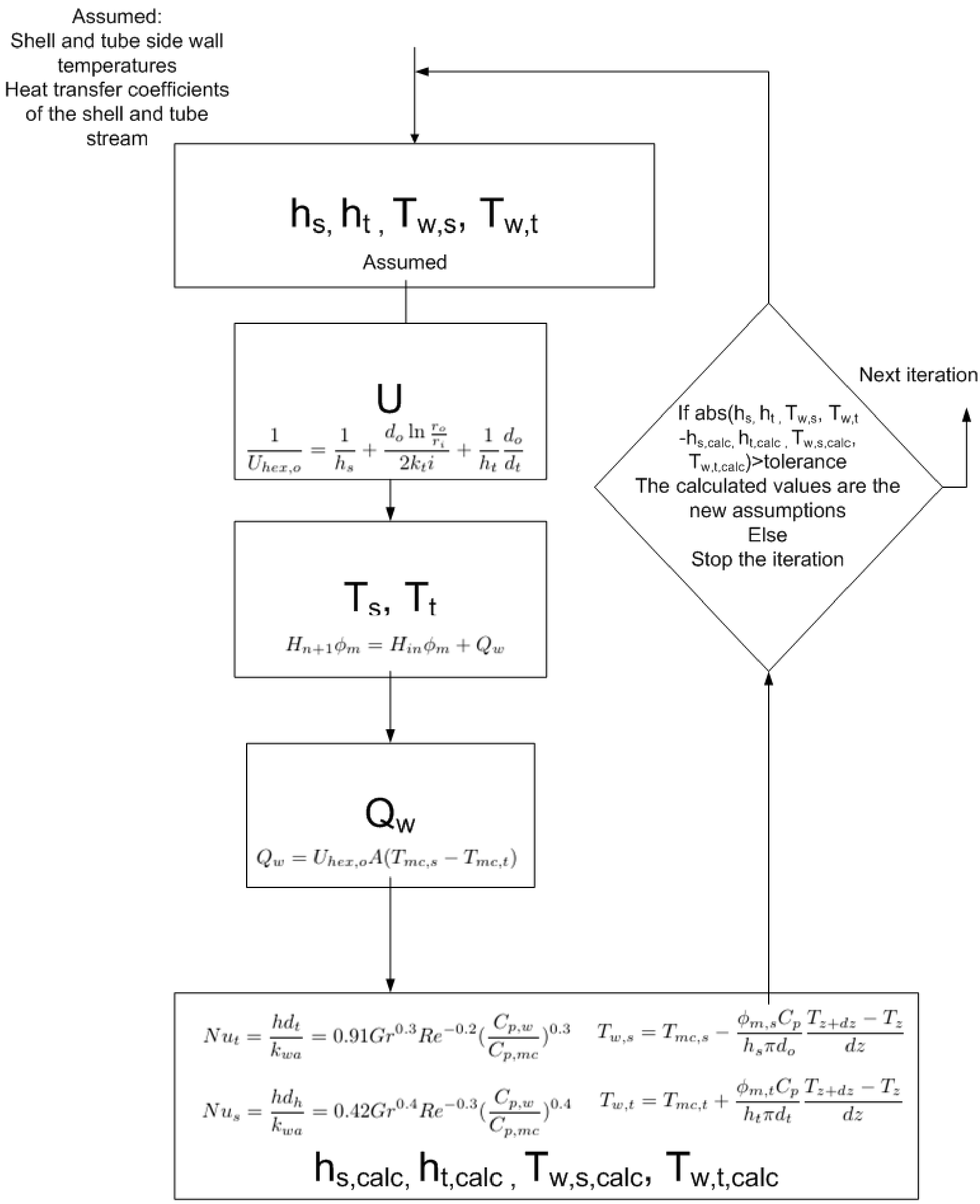

Figure 5: Iterative method for the heat exchanger of every axial section

The model is based on iteration steps. The heat exchanger is divided into an equal amount of sections. The temperature of the tube and shell streams are calculated from the enthalpy change due to the heat transfer from the wall. At the beginning of the model an educated guess of the shell and tube heat transport coefficients and the shell and tube side wall temperatures are made. The educated guess is the starting point for the iteration. The assumed values provide a starting point for the calculation of the heat through the wall, the shell and tube stream temperatures, the heat transfer coefficients and the inner wall tube and shell side temperatues. Each section is recalculated until the guessed heat transfer coefficients match the calculated values and the guessed inner wall temperatures match the calculated values. The calculated values become the new assumptions if they do not match the previous assumed values. Through iterations the entire inner wall temperature and heat transport coefficient profile is determined. The iterations for each section is shown as a block scheme in figure 5.

The heights of each section is fixed to a constant value. The area and height that is calculated for each section is the same. The heat flow varies for every section. The iterations are done until the pre-determined number of sections is reached, which determine the length of the heat exchanger. The inlet temperatures of the tube and shell are fixed before the simulation of the model starts. The flow is counter current. To start the iterations a guessed value of the outlet shell temperature is made. The guessed value provides the possibility to start the calculation at the same axial starting position. With the guessed outlet shell stream temperature the inlet shell stream temperature is determined. if it does not match the guessed value it is changed until the final value/ inlet shell stream temperature matches the pre-determined fixed value. This technique is based on the shooting method for numerical analysis. The explained theory is based on the hot shell and cold tube configuration. The hot tube and cold shell configuration has most of the same specifications, but differs in the heat balance. The heat is now transferred from the tube side to the shell side. The alternative formulas are depicted in equation (28), (29) and (30).

$$\frac{T_{z+dz} - T_z}{dz} = \frac{h_s \pi d_o}{\phi_{m,s} C_p}(T_{w,s} - T_{mc,s}) \tag{28}$$

$$\frac{T_{z+dz} - T_z}{dz} = \frac{-h_t \pi d_t}{\phi_{m,t} C_p}(T_{w,t} - T_{mc,t}) \tag{29}$$

$$U_{hex,o} = \frac{Q_w}{A(T_{mc,t} - T_{mc,s})} \tag{30}$$

6 Set-up description and experimental section

6.1 Experimental data of the heated tube

The Matlab model of the heated tube is based on the heat exchange apparatus shown in figure 6. The specifications are tabulated in table 2. The water inside the vertical tube flows from the bottom to the top. The electrical heating blocks ensure the outer wall temperature profile. The probe inside the tube measures the temperature at several radial positions, but all at the same axial position. It is not possible to measure the velocity profile inside the tube. The mixing cup temperature is modified (equation (31)) and used to predict the mean temperature of the different measured radial temperatures inside the tube. The probe inside the heated tube measures the temperature at one axial position. The probe can be moved through the column to measure at different axial positions.

$$T_{mc,mod} = \frac{\int_0^{r_t} T(r,z) C_p 2\pi r dr}{\int_0^{r_t} C_p 2\pi r dr} \tag{31}$$

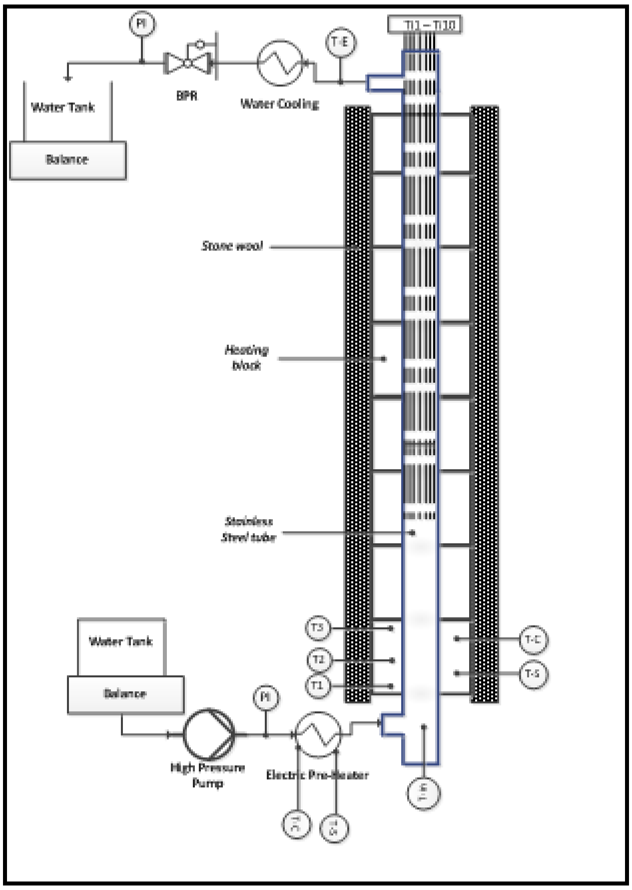

Figure 6: Experimental set up of the heated tube

Table 2: Specifications heated tube

Inner diameter	21.4	mm
Outer diameter	34.1	mm
Length	1.5	m
Maximum pressure	350	bar
Maximum temperature	500	°C

The 1D heated tube model is validated through results from the 2D Comsol calculations, experimental values from previous research and with newly done experiments. The Comsol model is already validated and the results can be used to validate the developed 1D Matlab model. The first three cases stated in table 3(resp. A, B and C) are obtained from the Comsol model. The second three cases tabulated in table 3 (resp. D, E and

F) are experimental values from previous work, without the inner wall temperatures [10]. The last two cases shown in table 3 (resp. G and H) are results obtained by own experiments for which the inner wall temperature was included.

Table 3: Case information

Case #	Mass flow [kg/hr]	Mass flux [$\frac{kg}{m^2 s}$]	Pressure [bar]	Inlet tempreature [°C]
A0	11.4	2.2	300	72
B0	8.0	1.6	300	85
C0	4.1	0.8	300	345.5
D0	8.0	1.6	303	86.4
E0	4.1	0.8	299	86.4
F0	11.4	2.2	301	72.5
G0	4.1	0.8	300	22.4
H0	8	1.6	300	21.9

6.2 Experimental data of the heat exchanger

The heat exchanger set up is shown in 7. The figure also indicates the dimensions of the heat exchanger set up. The figure shows the heat exchanger for the hot shell side stream and the cold tube side stream configuration. The heat exchanger set up is only able to measure the inlet and outlet temperatures of the heat exchanger. It is not possible to measure the temperature at axial positions inside the column.

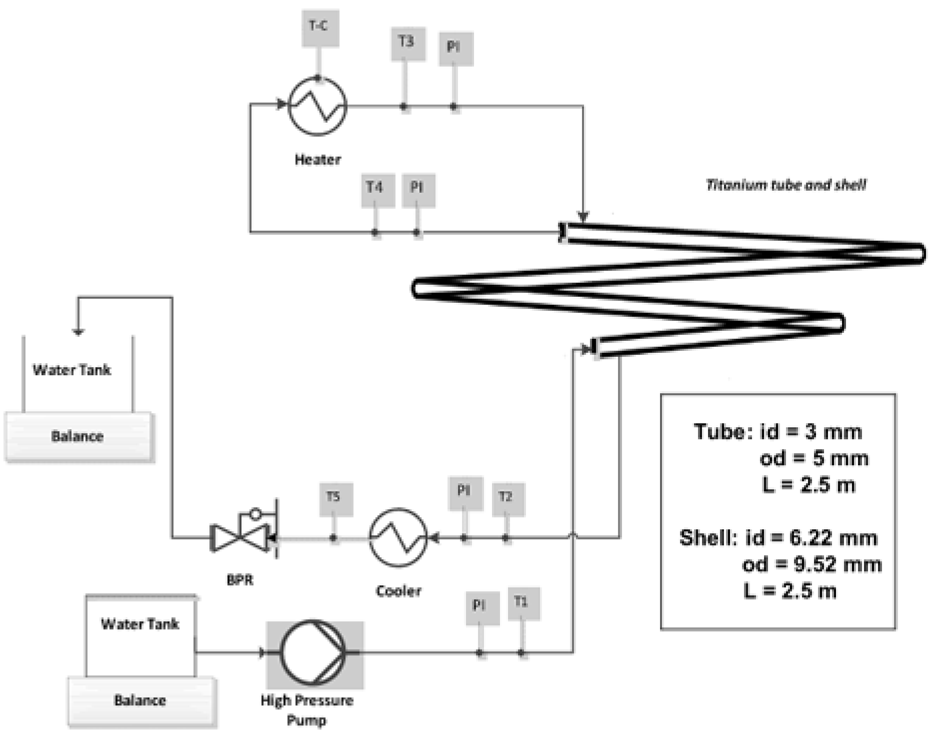

Figure 7: Experimental set up of the heat exchanger, hot shell/ cold tube configuration

The heat exchanger model is validated by experimental data. The specifications of the experiments are tabulated in table 4 and 5. For both the configurations eight cases are tabulated to validate the developed model.

Table 4: Experimental data Hot shell configuration

Case #	Mass flow [kg/hr]	Mass flux shell [$\frac{kg}{m^2s}$]	Mass flux tube [$\frac{kg}{m^2s}$]	pressure [bar]	Inlet temp. shell [°C]	Outlet temp. shell [°C]	Inlet temp. tube [°C]	Outlet temp. tube [°C]
A1	1.2	31.0	47.2	251	404.6	34.6	18.7	344.4
B1	1.2	31.0	47.2	251	422.3	55.9	18.6	345.0
C1	1.2	31.0	47.2	251	440.0	70.9	18.5	345.2
D1	1.2	31.0	47.2	251	460.6	69.7	18.5	345.2
E1	1.2	31.0	47.2	301	401.2	42.7	18.5	359.3
F1	1.2	31.0	47.2	301	420.1	37.5	18.5	359.7
G1	1.2	31.0	47.2	301	440.5	35.5	18.7	359.9
H1	1.2	31.0	47.2	301	460.9	34.4	18.5	359.9

Table 5: Experimental data Hot tube configuration

Case #	Mass flow [kg/hr]	Mass flux shell [$\frac{kg}{m^2s}$]	Mass flux tube [$\frac{kg}{m^2s}$]	pressure [bar]	Inlet temp. shell [°C]	Outlet temp. shell [°C]	Inlet temp. tube [°C]	Outlet temp. tube [°C]
A2	1.2	31.0	47.2	255	17.7	326.6	371.2	81.5
B2	1.2	31.0	47.2	255	17.9	340.1	441.8	99.5
C2	1.2	31.0	47.2	255	17.8	340.9	457.5	121.7
D2	1.2	31.0	47.2	255	17.7	340.5	471.7	128.9
E2	1.2	31.0	47.2	302	17.7	344.7	379.5	46.1
F2	1.2	31.0	47.2	302	17.6	355.7	444.9	63.1
G2	1.2	31.0	47.2	302	17.7	355.5	460.9	73.5
H2	1.2	31.0	47.2	302	17.7	355.0	474.0	82.2

7 Results and Discussion

The experimental data are compared with the simulated values from the numerical analysis of the heated tube and the heat exchanger. The experimental data is used to validate the Matlab models.

7.1 Heated tube

The heated tube is validated by eight cases. The data for the cases A, B and C are obtained from Comsol. The data of cases D, E and F are from previously done research. The last two cases, G and H, are from experiments done on the actual heated tube set up by myself. The new experiments are executed, because the literature values do not contain the inner wall temperature of the heated tube. The results of these cases are shown in appendix (chapter 12). The figures show the comparison between the simulated values from the model and the experimentally obtained data.

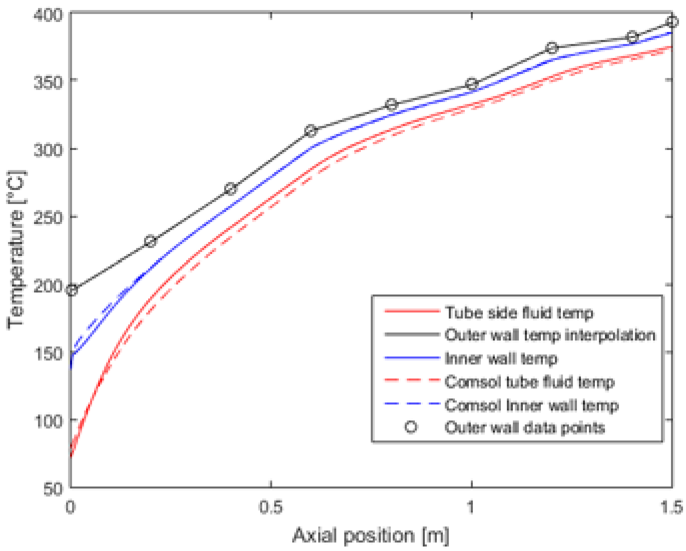

Figure 8: Case A

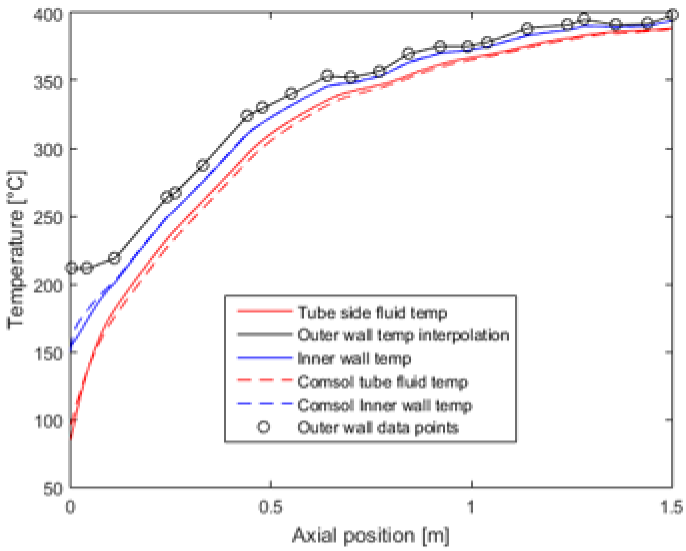

Figure 9: Case B

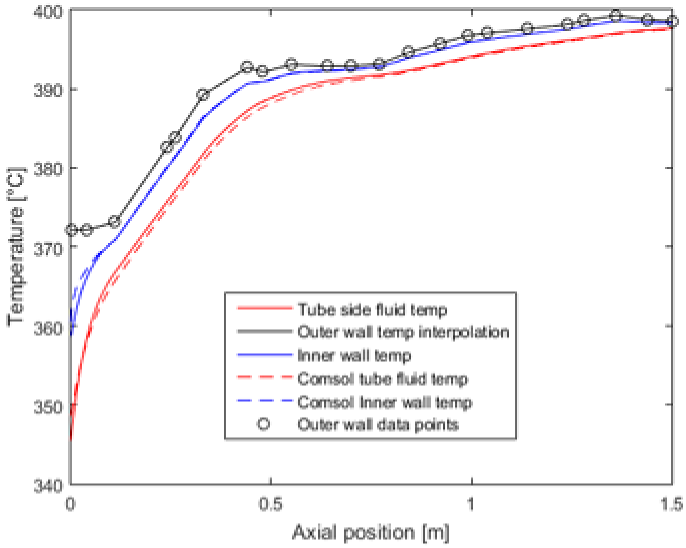

Figure 10: Case C

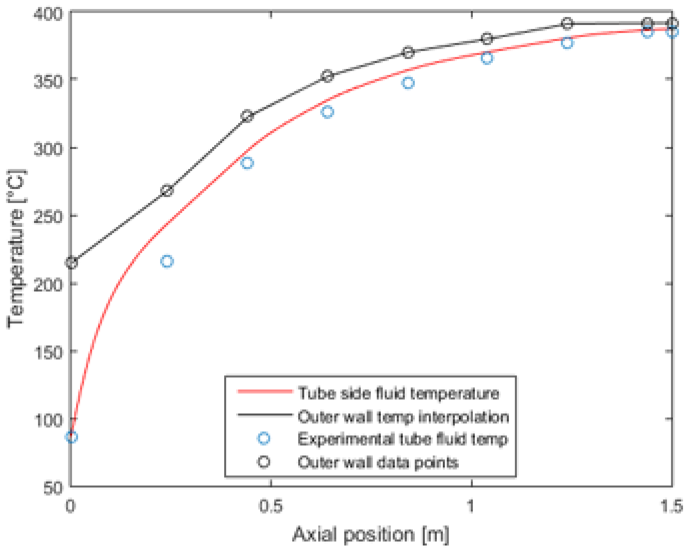

Figure 11: Case D

The heated tube model is validated with eight different cases. The developed model is based on the Nusselt correlation of equation 7, which is a critical factor in the predictions. The mass flux is kept below the 20 $\frac{kg}{m^2 s}$ in all eight cases. The experiments are also performed on a vertical tube. The same configuration as for which the correlation was obtained. The figures of appendix (chapter 12) show that the predicted values of the model correspond with the experimental data. The correlation is valid for a laminar flow.

For the cases D till H the number of experimental outer wall temperatures is low. Cases A, B and C are based on data points from Comsol which ensures more outer wall temperature data points. The outer wall profile is based on linear interpolation. The shape of the outer wall temperature will differ in the cases D till H if more outer wall temperature points are available. The error of the predicted values is dependent on the number of data points for the outer wall temperature. The heated tube model is based on iterations. The height of each iteration section determines the precision of the iterative method. Due to the various assumptions, the predicted values differ slightly from the experimental data. This slight deviation is present in all cases. The numerical analysis does not incorporate any form of heat loss. The wall is assumed to be fully insulated. In practice heat will flow to the surroundings. The figures of appendix (chapter12) show that there is only a slight deviation in the temperature profiles. This confirms the assumption that heat loss can be neglected.

The experimental temperatures of cases A till C are based on the mixing cup temperatures calculated by Comsol, equation 2. The numerical calculations of the Matlab temperatures are also the mixing cup temperatures. The mixing cup temperature is based on the radial velocity profile. It is not possible to measure the velocity profile with the experimental heated tube set up. The mixing cup temperature is approached by the modified mixing cup temperature, equation 31. At lower axial positions the radial velocity gradient is larger. This causes a difference between the modified mixing cup temperature of the experiments and the predicted temperature of the model. Cases D till H show this deviation at the lower positions. The deviation decreases with the increasing axial position. At the axial position of 33 cm in cases G and H the experimental value is off. This is likely caused by the developing of the flow. At the beginning of the column the flow needs time to develop the profile and to become constant. At a lower mass flow the development is finished at an earlier axial position. This can also be seen in case G in comparison with case H. The experimental values are better matching because the flow will stop developing at a lower axial position.

7.2 Heat exchanger

The results of the heat exchanger are tabulated in table 6 and 7. For two cases the temperature profiles of the heat exchanger simulations are shown in figure 12,13,14 & 15. The figures for all the different cases are shown in appendix (chapter 13 and 14). The case numbering matches the numbering of table 7 and 6. The figures are simulated with and without heat loss. The heat flow inside the tube and shell streams of the model are calculated with the heat balance of equation 22. The heat loss to the environment is implemented in the model. The shell side is in direct contact with the surroundings, through which the heat is lost. The heat loss varies inside the column and is dependent on the temperatures that are present. To mimic the heat loss profile a percentage of the heat flow from the wall is lost. The heat loss percentage can be adjusted for every case to obtain the right absolute heat loss value. The heat loss of the experimental set up is determined by enthalpy calculations for the inlet and outlet flow conditions performed with XSteam [1]. During the design of a heat exchanger the amount of heat loss is unknown. The heat loss is used to compare and validate the simulation results with the experimental values. Due to the small scale of the set up the heat loss can not be neglected.

Table 6: Experimental data hot shell configuration

Case #	Type	Inlet temp. shell [°C]	Outlet temp. shell [°C]	Inlet temp. tube [°C]	Outlet temp. tube [°C]	Heat loss [W]	Heat loss [%]
A1	Experiment	404.6	34.6	18.7	344.4	330	40.3
A1	Model, no heat loss	404.2	104.1	18.7	387.1	0	0
A1	Model, with heat loss	404.0	28.0	18.7	345.1	330.6	40
B1	Experiment	422.3	55.9	18.6	345.1	340	40.5
B1	Model, no heat loss	421.8	112.9	18.6	390.2	0	0
B1	Model, with heat loss	421.8	29.0	18.6	361.3	342.4	39
C1	Experiment	440.0	70.9	18.5	345.2	360	41.9
C1	Model, no heat loss	439.2	118.6	18.5	393.9	0	0
C1	Model, with heat loss	439.4	29.2	18.5	365.6	366	40
D1	Experiment	460.6	69.7	18.5	345.2	400	44.4
D1	Model, no heat loss	461.2	124.1	18.5	399.5	0	0
D1	Model, with heat loss	460.0	29.0	18.5	366.7	399.3	40
E1	Experiment	401.2	42.7	18.5	359.2	140	21.2
E1	Model, no heat loss	402.1	59.1	18.5	395.0	0	0
E1	Model, with heat loss	400.7	31.3	18.5	362.1	140.4	21
F1	Experiment	420.1	37.5	18.5	359.7	270	34.2
F1	Model, no heat loss	420.5	80.1	18.5	406.0	0	0
F1	Model, with heat loss	420.2	28.5	18.5	362.5	272.4	34
G1	Experiment	440.5	35.4	18.6	359.9	340	39.5
G1	Model, no heat loss	439.5	90.2	18.6	413.2	0	0
G1	Model, with heat loss	441.4	28.0	18.6	363.4	339.4	39
H1	Experiment	460.9	34.4	18.5	359.9	390	42.9
H1	Model, no heat loss	460.1	97.1	18.5	420.8	0	0
H1	Model, with heat loss	460.7	27.6	18.5	363.0	383.9	42

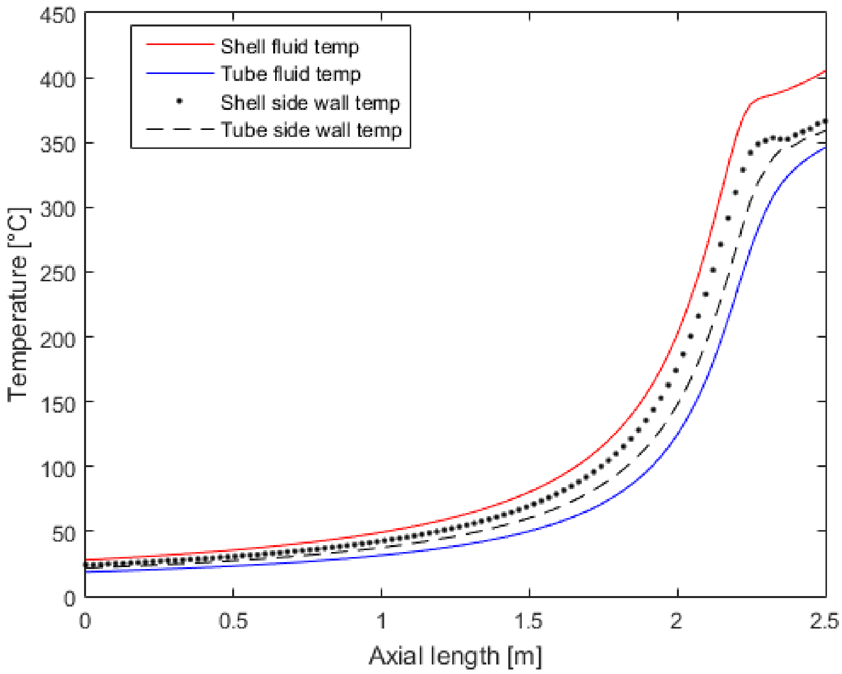

Figure 12: Case A1 hot shell configuration with heat loss

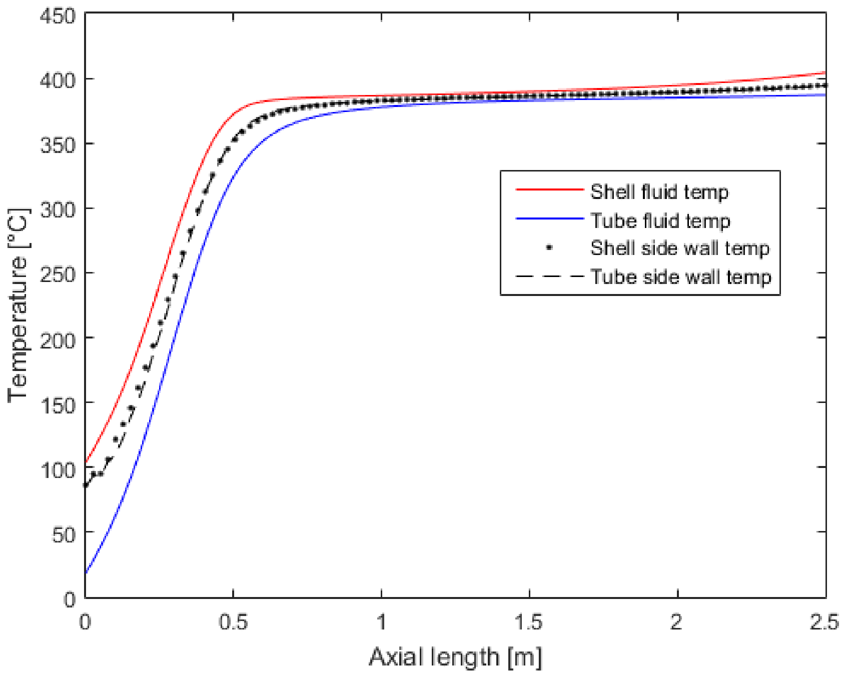

Figure 13: Case A1 hot shell configuration with no heat loss

Table 7: Experimental data hot tube configuration

Case #	Type	Inlet temp. shell [°C]	Outlet temp. shell [°C]	Inlet temp. tube [°C]	Outlet temp. tube [°C]	Heat loss [W]	Heat loss [%]
A2	Experiment	17.7	326.6	371.2	81.5	20	4.2
A2	Model, no heat loss	17.7	356.5	370.9	48.0	0	0
A2	Model, with heat loss	17.7	351.2	371.1	42.5	21	4
B2	Experiment	17.9	340.1	441.8	99.5	330	40.2
B2	Model, no heat loss	17.9	393.6	440.6	127.9	0	0
B2	Model, with heat loss	17.9	375.3	441.0	33.2	327	36
C2	Experiment	17.8	340.9	457.5	121.9	330	40.2
C2	Model, no heat loss	17.8	397.0	457.3	132.9	0	0
C2	Model, with heat loss	17.8	380.4	457.1	34.5	327	35
D2	Experiment	17.7	340.5	471.7	128.1	340	41.0
D2	Model, no heat loss	17.7	400.0	470.6	136.1	0	0
D2	Model, with heat loss	17.7	382.4	472.6	35.1	335	35
E2	Experiment	17.7	344.7	379.5	46.1	50	9.3
E2	Model, no heat loss	17.7	363.2	378.6	48.2	0	0
E2	Model, with heat loss	17.7	348.4	379.0	37.5	49	9
F2	Experiment	17.6	355.7	444.9	63.1	320	38.6
F2	Model, no heat loss	17.6	413.5	445.3	99.1	0	0
F2	Model, with heat loss	17.6	371.4	445.4	29.6	324	37
G2	Experiment	17.7	355.5	460.9	73.5	340	40.0
G2	Model, no heat loss	17.7	418.7	461.1	105.1	0	0
G2	Model, with heat loss	17.7	375.1	459.7	29.9	345	38
H2	Experiment	17.7	355.0	474.0	82.2	350	40.7
H2	Model, no heat loss	17.7	422.7	472.9	108.7	0	0
H2	Model, with heat loss	17.7	380.3	473.6	30.4	354	38

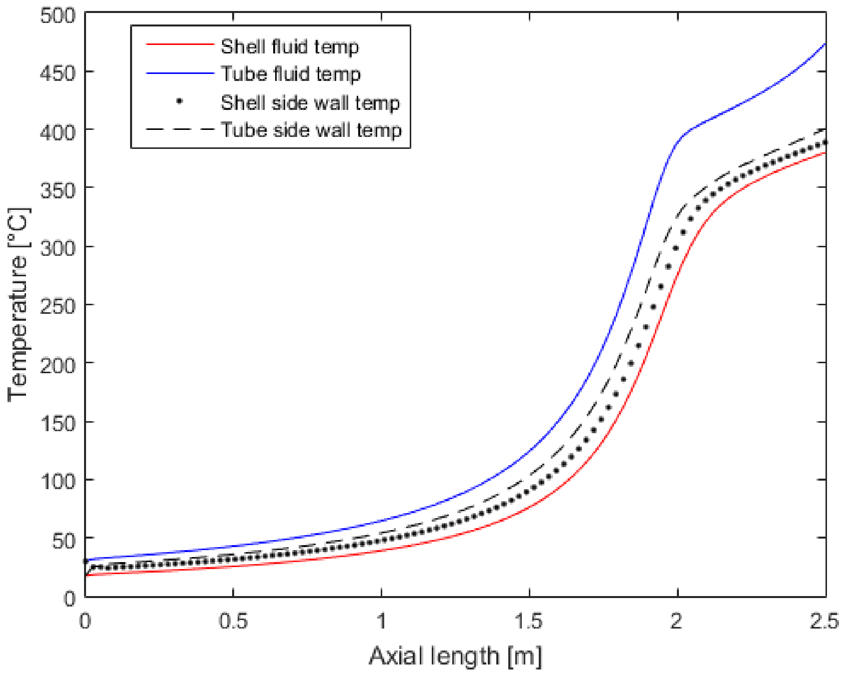

Figure 14: Case H2 hot tube configuration with heat loss

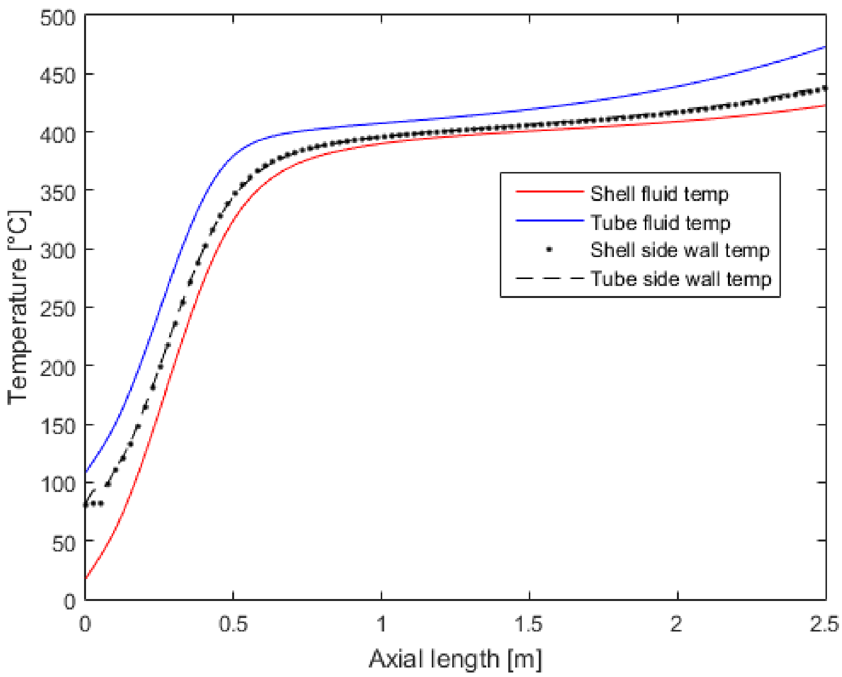

Figure 15: Case H2 hot tube configuration with no heat loss

Table 8 shows the results for different percentages heat loss. The accompanying graphs are shown in figure 38, 16, 17 and 37. The heat loss is calculated by substracting the heat loss percentage from the heat flow throug the wall, equation 22. The results show that above a percentage of 10 % the temperature profile changes. The heat loss profile along the axial direction is unknown. The percentage method is used as a prediction for the heat loss per section. The results indicate that the influence of the percentage is higher at lower temperatures. The percentage heat loss in the numerical analysis is adjusted until the absolute heat loss matches the experimental value. The overall heat loss is thus the same. The inlet and outlet temperatures can therefore be used for the design, but the actual temperature profile can be different then what the simulation calculates.

Table 8: Experimental data hot shell configuration with heat loss effect for case H1

Case #	Type	Inlet temp. shell [°C]	Outlet temp. shell [°C]	Inlet temp. tube [°C]	Outlet temp. tube [°C]	Heat loss [W]	Heat loss [%]
H1	Model, no heat loss	460.1	97.1	18.5	420.8	0	0
H1	Model	460.4	60.5	18.5	413.4	86.8	10
H1	Model	460.4	39.2	18.5	404.4	179.4	20
H1	Model	460.7	27.6	18.5	363.0	383.9	42

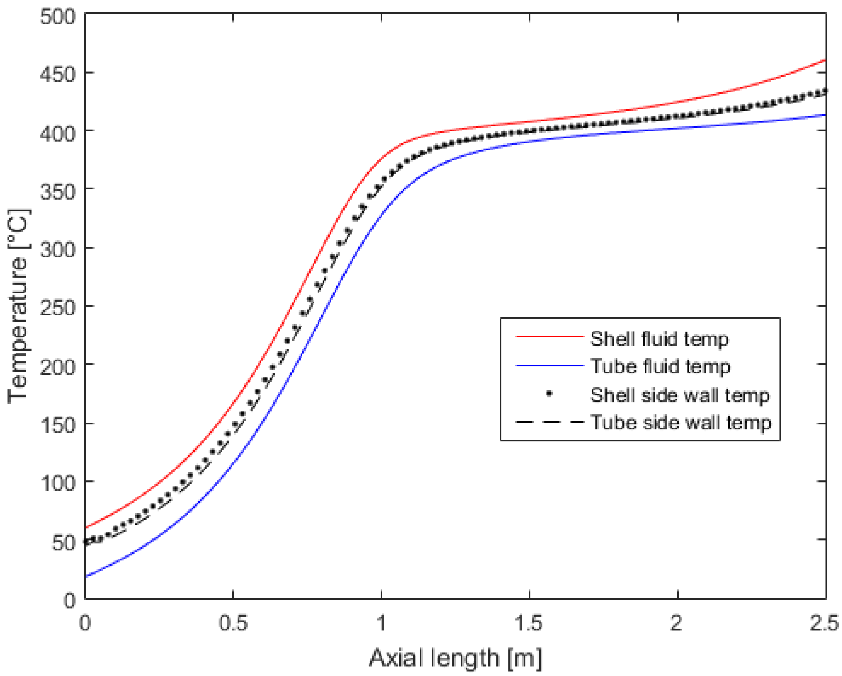

Figure 16: Case H1 hot shell configuration with 10% heat loss

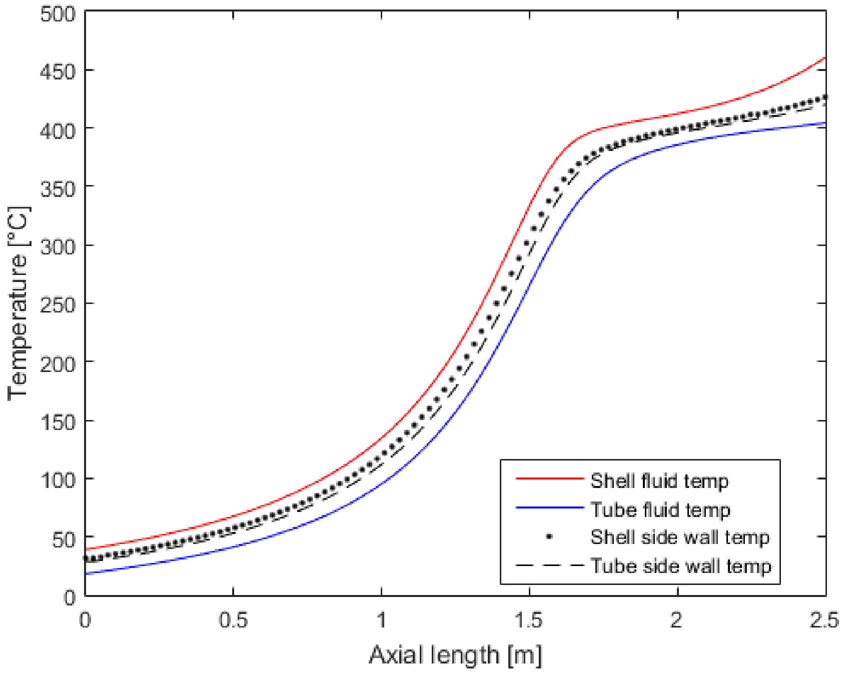

Figure 17: Case H1 hot shell configuration with 20 % heat loss

The shape for the temperature profiles with a heat loss above the 10 % shows a irregular shape in comparison with the zero heat loss simulation. The shape of the larger heat loss percentages is checked by the heat transfer coefficient, figure 18. The curve of the heat transfer coefficient show that the temperature profiles are in agreement with the heat transfer coefficients. The problem with the temperature profiles is probably due to the heat loss implementation.

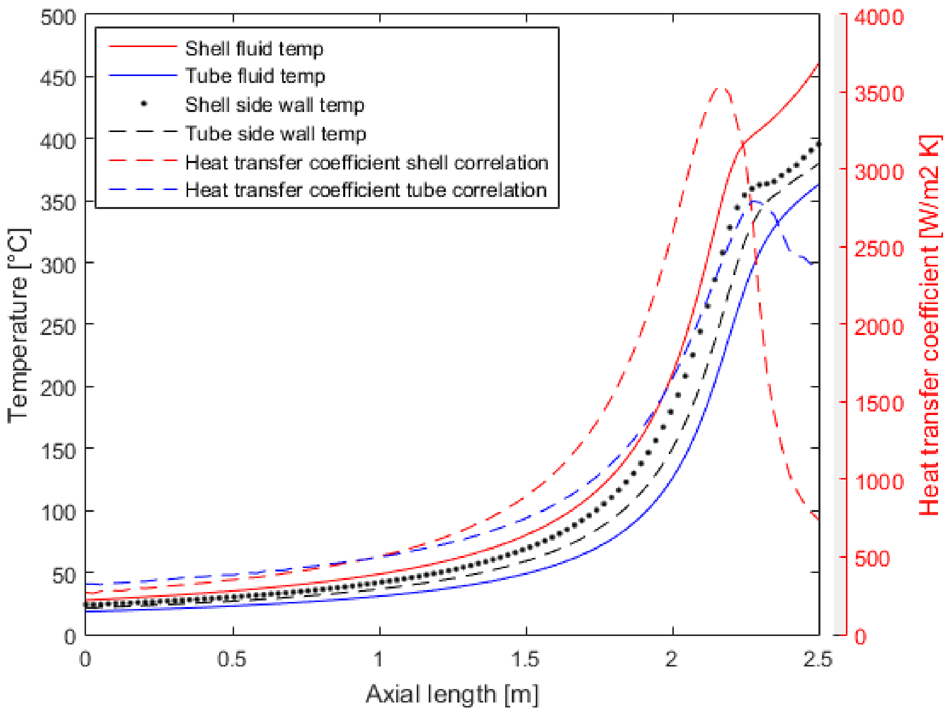

Figure 18: Case H1 hot shell configuration with the temperature and heat transfer coefficient profile

The numerical calculations show that the Nusselt correlation that is used over predicts the outlet temperatures of the tube and shell. The boundary conditions of the correlations are not met (table 1). The Nusselt correlation for a similar tube length is shown in appendix (chapter15). The shape of the heat transfer coefficients from Comsol and the heat exchanger model are in agreement with each other, but it also indicates that the values are over predicted. To compensate for the over prediction the used Nusselt correlation is multiplied by a factor of 0.8. The results of appendix (chapter 15) show that the heat transfer coefficient is roughly 20 % over predicting. So the Nusselt correlation is compensating with a factor 0.8. The results of these calculations are tabulated in table 9. The numerical calculations are in better agreement with the experimental values, but still show a deviation. For the hot shell/ cold tube configuration the deviation is 20 % in the shell and 1 % in the tube. The modification of the Nusselt correlation results in a deviation of 10 % in the shell and 0.5 % in the tube. The deviation for the hot tube/ cold shell configuration is larger. The tube side has a deviation of 57 % and the shell side 7 %. The modified Nusselt correlation results in a smaller deviation. The tube side deviation is 55 % and the shell side 6 %. Decreasing the Nusselt correlation results with a constant value will arguably not give a solution which is in agreement with experiments.

Table 9: Calculations for the difference in Nusselt correlations

Case #	Type	Inlet temp. shell [°C]	Outlet temp. shell [°C]	Inlet temp. tube [°C]	Outlet temp. tube [°C]	Heat loss [W]	Heat loss [%]
G1	Experiment	440.5	35.4	18.6	359.9	340	39.5
G1	Model, 0.8 Nusselt	439.9	31.6	18.6	361.1	336.1	39
G1	Model	441.4	28.0	18.6	363.4	339.4	39
H1	Experiment	460.9	34.4	18.5	359.9	390	42.9
H1	Model, 0.8 Nusselt	460.8	31.3	18.5	361.8	382	42
H1	Model	460.7	27.6	18.5	363.0	383.9	42
G2	Experiment	17.7	355.5	460.9	73.5	340	40.7
G2	Model, 0.8 Nusselt	17.7	374.4	461.3	34.8	343.8	38
G2	Model	17.7	375.1	459.7	29.9	345	38
H2	Experiment	17.7	355.0	474.0	82.2	350	40
H2	Model, 0.8 Nusselt	17.7	378.6	472.6	35.3	351.4	38
H2	Model	17.7	380.3	473.6	30.4	354	38

The numerical analysis of the heat exchanger model for both configuration show a large deviation from the experimental data. The proposed reason is the validation of the Nusselt correlations, equation 8 and 7, which are used in model. The boundary conditions for which the correlations are valid are not met. The heat exchanger operates at a mass flux between 30 $\frac{kg}{m^2 s}$ and 50 $\frac{kg}{m^2 s}$. The experimental set up has a spiral heat exchanger. The diameter of the tube and shell are smaller in size then values for which the correlation is valid. The results of table 7 and 6 show that the model over predicts the outlet temperatures of the tube and shell stream. A 2D Comsol model is evaluated to check the heat transfer coefficient. The results of the 2D Comsol model are shown in appendix (chapter 14). The graphs of figure 58 and 55 show that the correlation is over predicting the heat transfer coefficient. This means that the heat exchange in the model is simulating a better heat exchange then experiments would measure. This strengthens the proposed reason that the correlation is off.

The hot tube/ cold shell configuration results of table 7 show that the simulated values have a very large deviation in comparison with the experimental data. The results of the second configuration with a cold tube/ hot shell in table 6 show the results are in better agreement, but still have a deviation. The Reynolds number inside the tube stream is higher then the shell stream due to the design dimensions. The Reynolds number is also temperature dependent and will increase with temperature. The hot stream inside the tube causes the Reynolds to be larger then if the tube contained the cold stream. The difference in Reynolds number caused by the different configuration are assumed to be the reason for the difference in deviation between the results.

8 Conclusion

The developed models for the heated tube and the heat exchanger are based on the Nusselt correlation, 7 and 8. The results of the heated tube are depicted in appendix (chapter12) and the results of the heat exchanger in table 6 and 7. The heated tube operating parameters are within the boundary conditions (table 1) of the Nusselt correlation and are in agreement with the simulated values. The mass flow inside the tube influences the flow development. The results from appendix (chapter 12) show that with a higher mass flow the flow development finishes at a higher axial position. Although the outlet temperature of the tube is in all cases in agreement with the experimental value. The flow development probably only influences the temperature profile inside the tube.

The heat exchanger operatings parameters are outside the boundary conditions of the Nusselt correlations and the numerical calculations show a deviation from the experimental values. The used Nusselt correlations over predicts the heat transfer inside the shell and tube. The incorporated heat loss has a positive effect on the validation, but is still not sufficient, table 8. Probably the used Nusselt correlation is the major contributor in the deviation. The major deviation is in the guessed value. For the first configuration the deviation goes from 20 % to 10 % by changing the Nusselt correlation. Changing the Nusselt correlation for the second configuration is of less influence and the deviation differs from 57 % to 55 %.

9 Recommendations

The heat exchanger model can not be validated through the experimentally obtained data. The configurations of the set up are not sufficient for measurements at lower mass fluxes or a lower Reynolds number. In the future, tests on a different set up need to be reviewed for the validation. These experiments should include a new experimental set up with a larger diameter, lower mass flux possibilities and a vertical shell and tube.

The other possibility is researching the used Nusselt correlations, equation 7 and 8, and modifying the used constants. The already used factor of 0.8, table 9, show that only multiplying it with a single factor is not sufficient. The in and outlet temperatures of the heat exchanger are measured experimentally, but this does not give an estimation about the temperature profile inside the column. To validate the numerical calculated temperature profiles it is usefull to incorporate the experimental measured temperatures at various axial positions.

The heat loss should be measured between different axial positions. This gives the opportunity to implement a heat loss profile along the axial direction. The heat loss per section is now calculated through a percentage of the heat flow through the wall. Results show that this has a large influence on the temperature profile.

The already validated model of the heated tube and the yet to validate heat exchanger model can be used in the scale up of both the heat exchange apparatusses. The scale increment of the models should be possible within the boundary conditions of the Nusselt number and would propose a usefull method in the design of supercritical processes.

References

[1] M. Holmgren. X steam for matlab. `www.x-eng.com`, januari 2006. Matlab data series for the physical properties of water.

[2] 'H Weingartner, E U Franck, G Wiegand, N Dahmen, G Schwedt, F H Frimmel, and B G Gordalla'. "water, 1. properties, analysis and hydrological cycle". *"Ullmann encyclopedia of industrial chemistry"*, "2012".

[3] Zhenxing Zhao and Defu Che. Numerical investigation of conjugate heat transfer to supercritical co2 in a vertical tube-in-tube heat exchanger. *An International Journal of Computation and Methodology*, 67:8, 2014.

[4] S.O. Odu, A.G.J. van der Ham, S.R.A. Kersten, and S. Metz. Design of a process for supercritical water desalination with zero liquid discharge. *Ind. Eng. Chem. Res.*, 54, 2015.

[5] N. Boukis, U. Galia, H. Müller, and E. Dinjus. Biomass gasification in supercritical water experimental progress achieved with the verena pilot plant. *15th European Biomass conference & exhibition*, 54, 2007.

[6] V. V. Slesarenko. Heat pumps as a source of heat energy for desalination of seawater. *Presented at the European Conference on Desalination and the Environment: Water Shortage, Lemesos, Cyprus*, 139, 2001.

[7] P. Koster. Numerical analysis of heat transfer in supercritical water at low mass flux mixed convection conditions. Master's thesis, 2014.

[8] Sarah Mokrya, Igor Pioro, Amjad Farah, Krysten King, Sahil Gupta, Wargha Peiman, and Pavel Kirillov. Development of supercritical water heat-transfer correlation for vertical bare tubes. *241*, Nuclear Engineering and Design, 2010.

[9] X. Cheng and T. Schulenberg. Heat transfer at supercritical pressures - literature review and application to an hplwr. Forschungszentrum Karlsruhe, 2001.

[10] R. Alaaeldin. Heat transfer measurements for supercritical water flow in a vertical tube at low mass fluxes. Master's thesis, 2015.

[11] M. van der Hoef and M van Sint Annaland J Kuipers. *Introduction to physical transport phenomena.* University of Twente, 2013.

[12] P C Simoes and J P Mota. Dynamic model of a supercritical carbon dioxide heat exchanger. *Journal of supercritical fluids*, 35, 2005.

[13] W. Brilman. *Physical transport phenomena.* University of Twente, 2014.

[14] R.K. Sinnott. *Chemical engineering design.* ELSEVIER, 2013.

[15] Comsol inc. Comsol. `http://www.comsol.com/`, 2015.

10 List of symbols

Nomenclature

β	Cubic expansion coefficient $[K^{-1}]$
η	Dynamic viscosity [Pa.s]
ϕ_m	Mass flow inside the tube $[\frac{kg}{s}]$
ρ	Density $[\frac{kg}{m^3}]$
A	Area $[m^2]$
C_p	Heat capacity $[\frac{J}{kgK}]$
d	Diameter [m]
G	Mass flux $[\frac{kg}{m^2s}]$
g	Specific gravitiy $[\frac{m}{s^2}]$
Gr	Grashof number [-]
H	Enthalpy $[\frac{kJ}{kg}]$
h	Heat transfer coefficient $[\frac{W}{m^2K}]$
k	Thermal conductivity $[\frac{W}{mK}]$
Nu	Nusselt number [-]
Pr	Prandtl number [-]
Q	Heat flow [W]
r	Radius [m]
Ra	Rayleigh number [-]
Re	Reynolds number [-]
T	Temperature [°C]
U	Overall heat transfer coefficient $[\frac{W}{m^2K}]$
z	Axial length [m]
n	Number of axial sections

11 Abbreviations

t	Tube side
o	Outer tube
w	Wall
s	Shell side
in	Inlet position
out	Outlet position
mc	Mixing cup
st	Stainless steel
wa	Water
tot	Total
av	Average
h	Hydraulic
ti	Titanium
hex	Heat exchanger
lm	Logaritmic mean
mod	Modified

12 Appendix 1 - Heated tube model

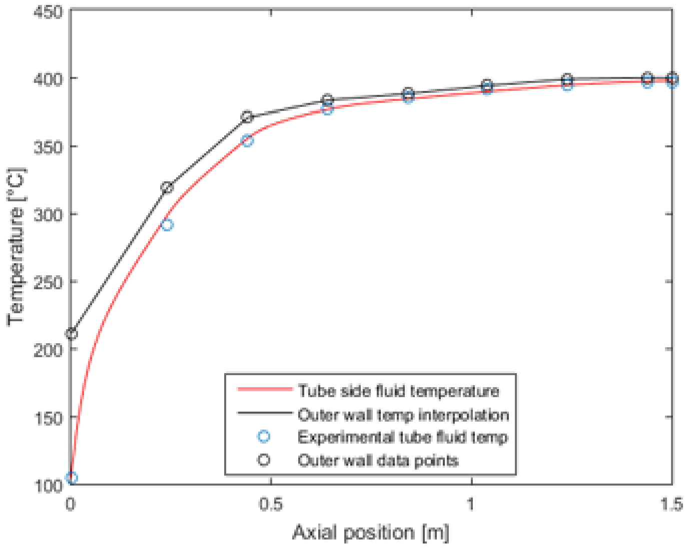

Figure 19: Case E

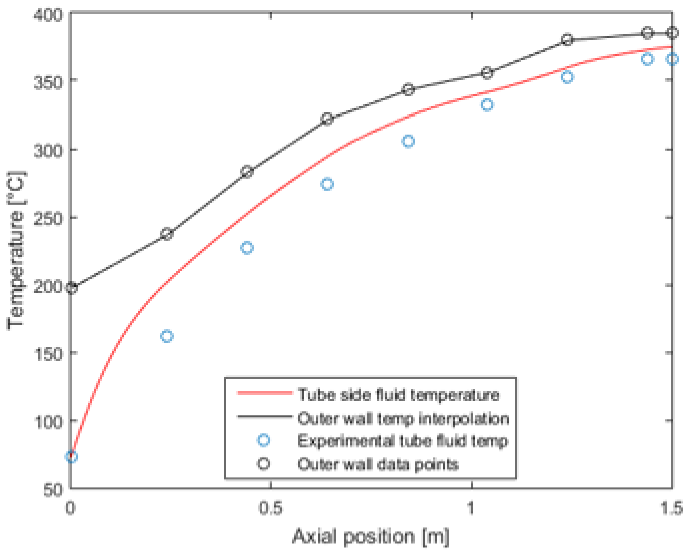

Figure 20: Case F

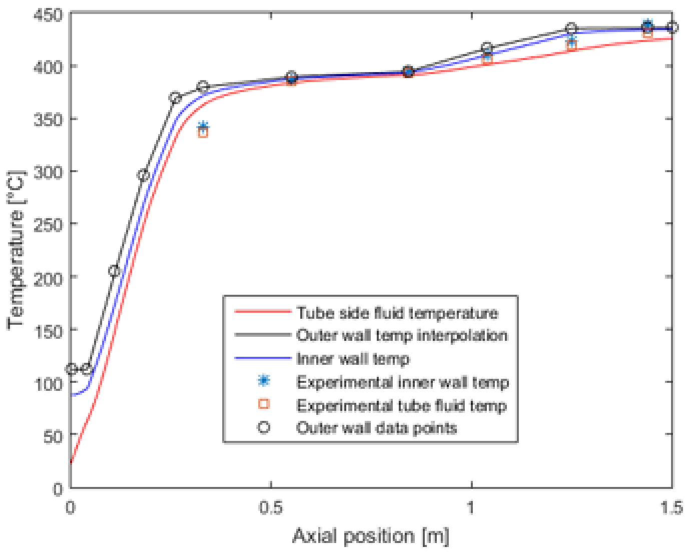

Figure 21: Case G

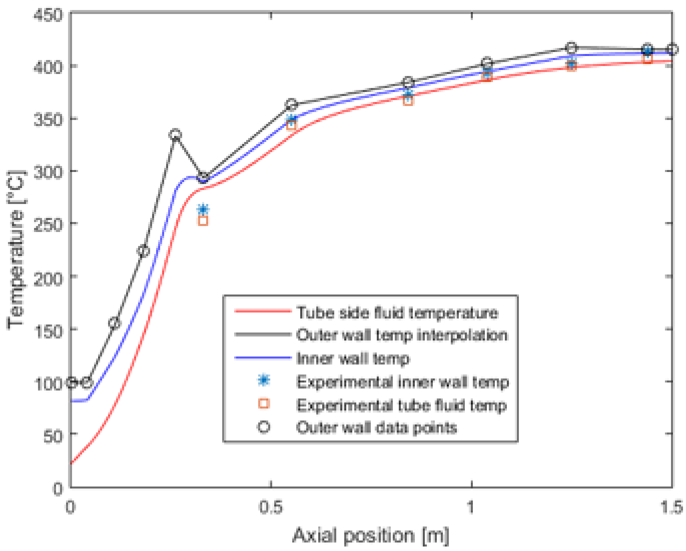

Figure 22: Case H

13 Appendix 2 - Heat exchanger model, hot shell/ cold tube

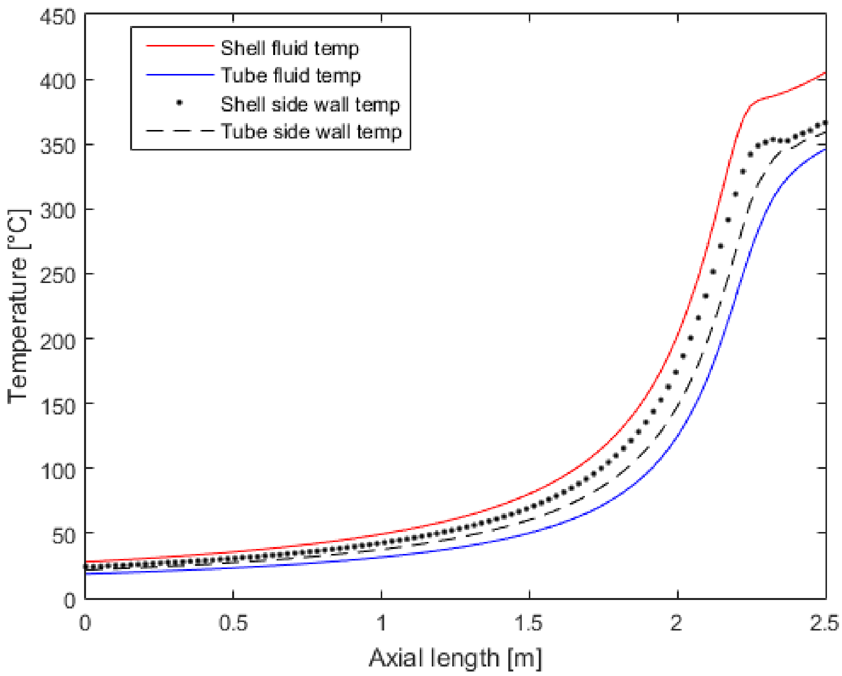

Figure 23: Case A1 hot shell configuration with heat loss

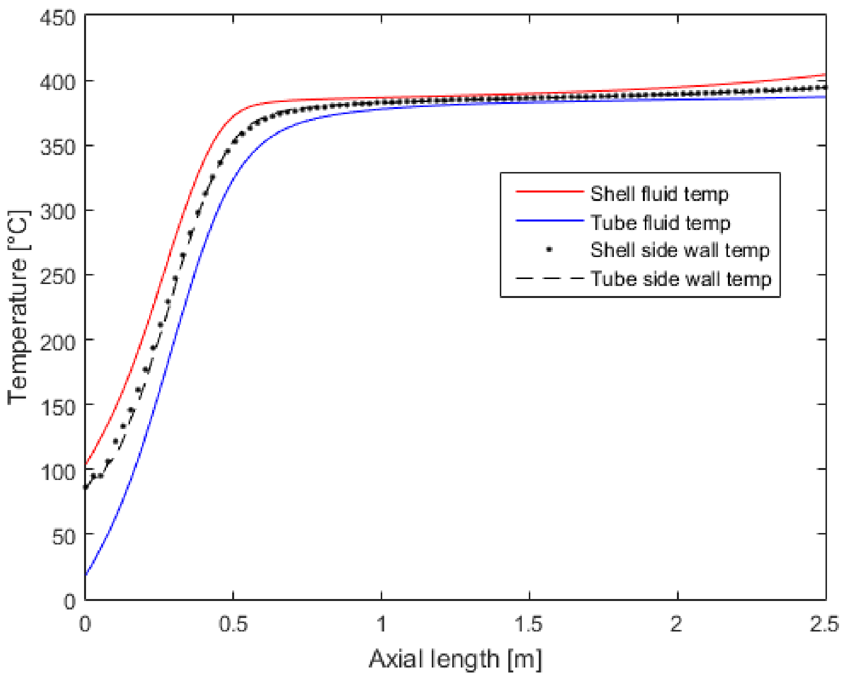

Figure 24: Case A1 hot shell configuration with no heat loss

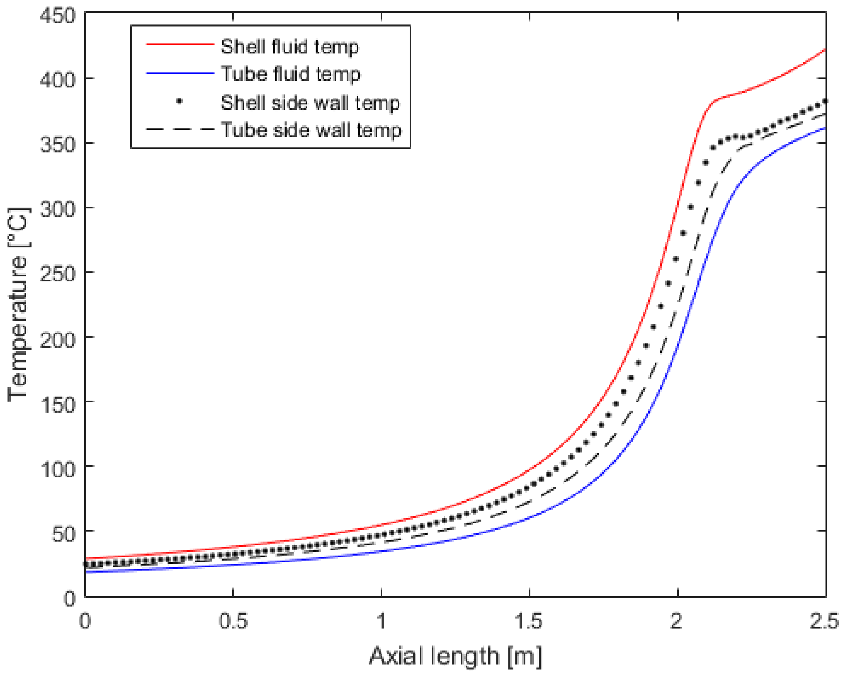

Figure 25: Case B1 hot shell configuration with heat loss

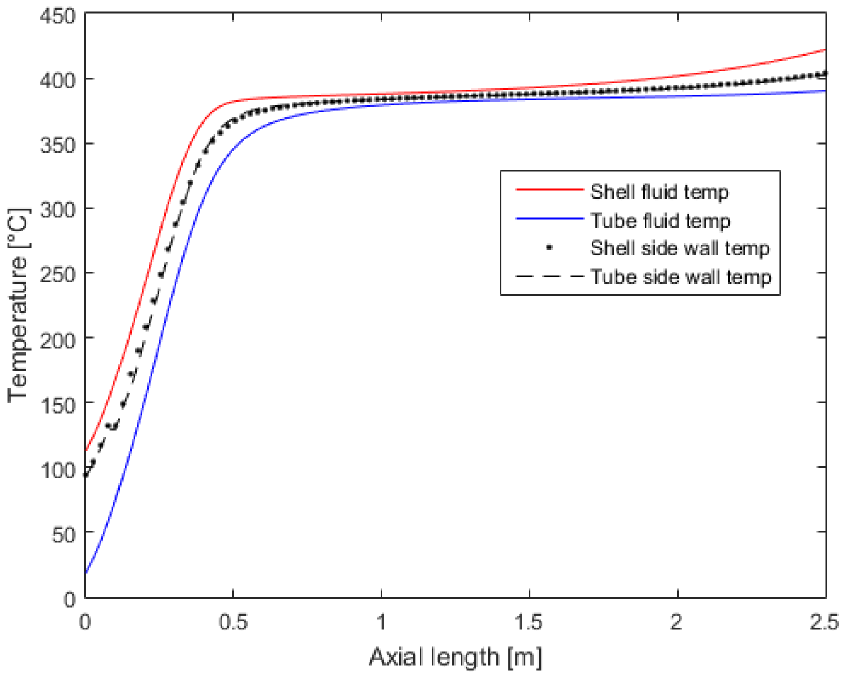

Figure 26: Case B1 hot shell configuration with no heat loss

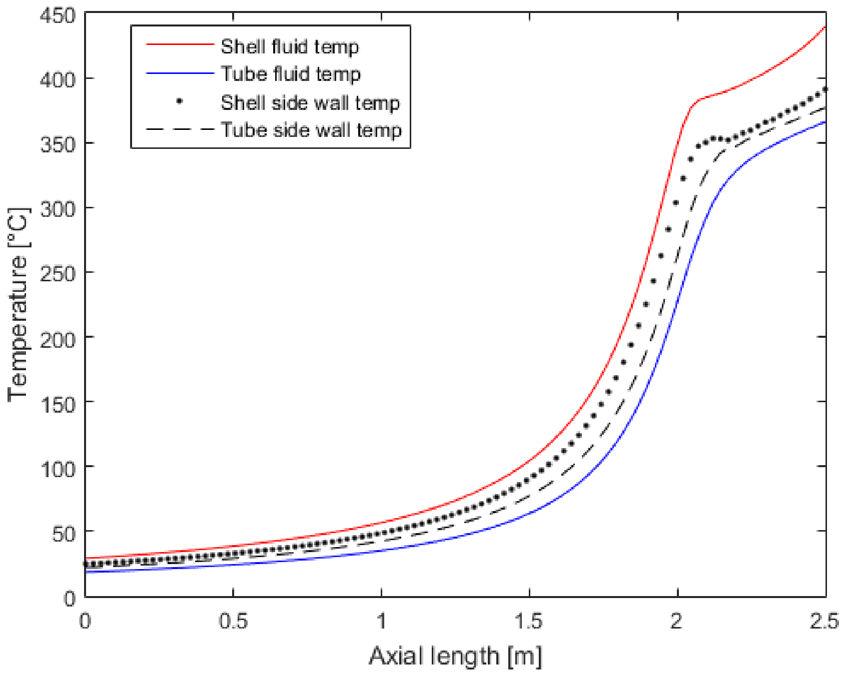

Figure 27: Case C1 hot shell configuration with heat loss

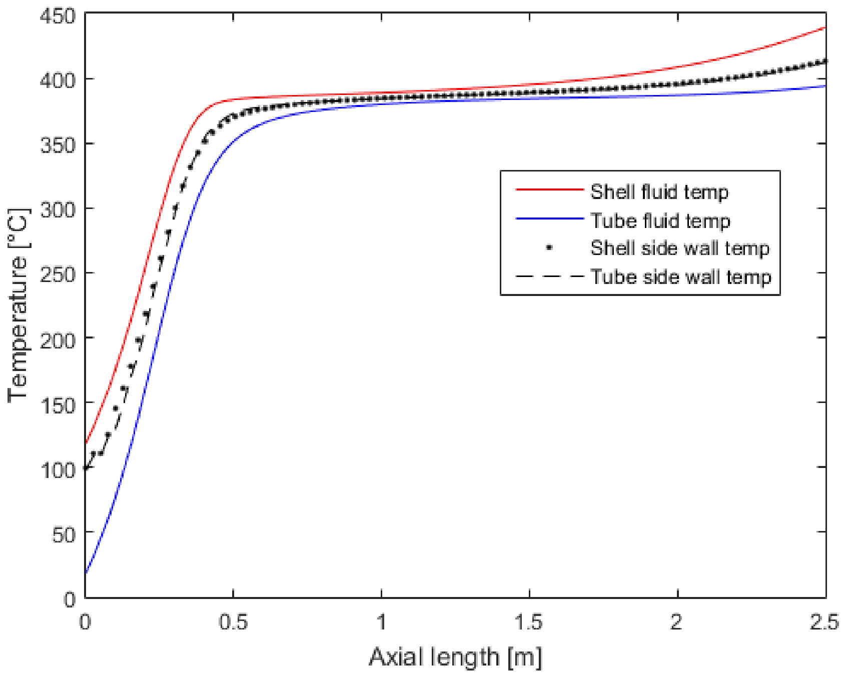

Figure 28: Case C1 hot shell configuration with no heat loss

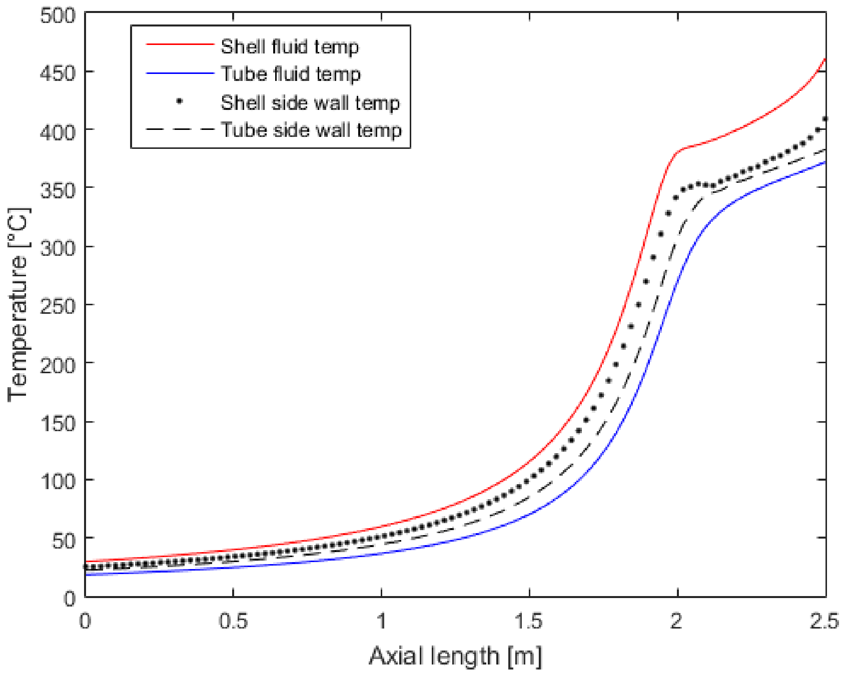

Figure 29: Case D1 hot Shell configuration with heat loss

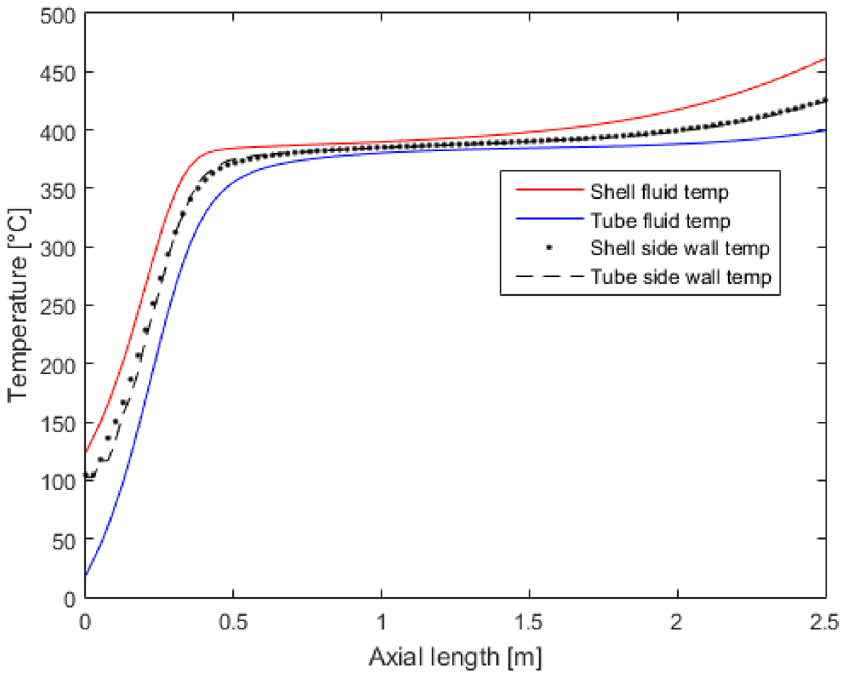

Figure 30: Case D1 hot Shell configuration with no heat loss

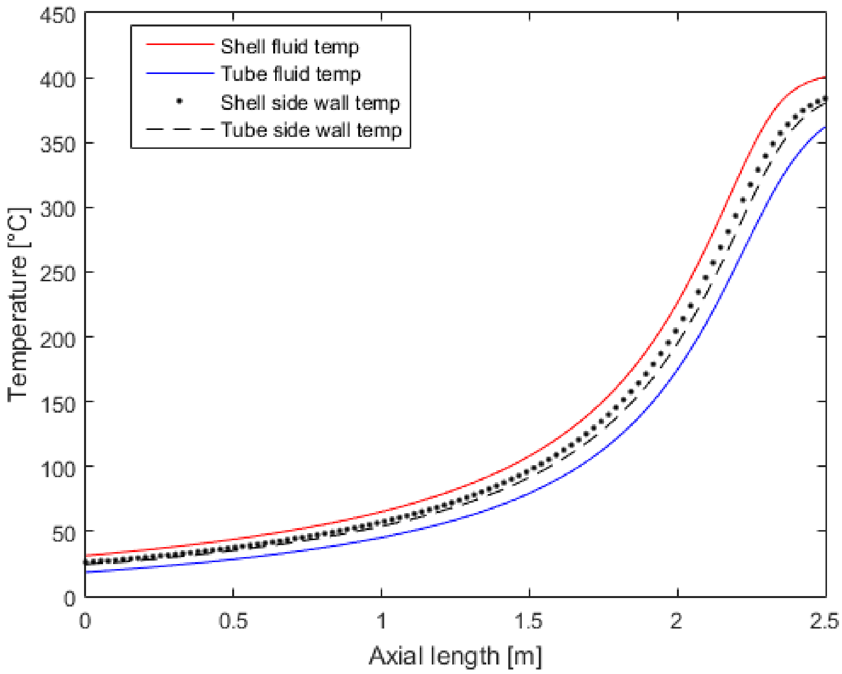

Figure 31: Case E1 hot shell configuration with heat loss

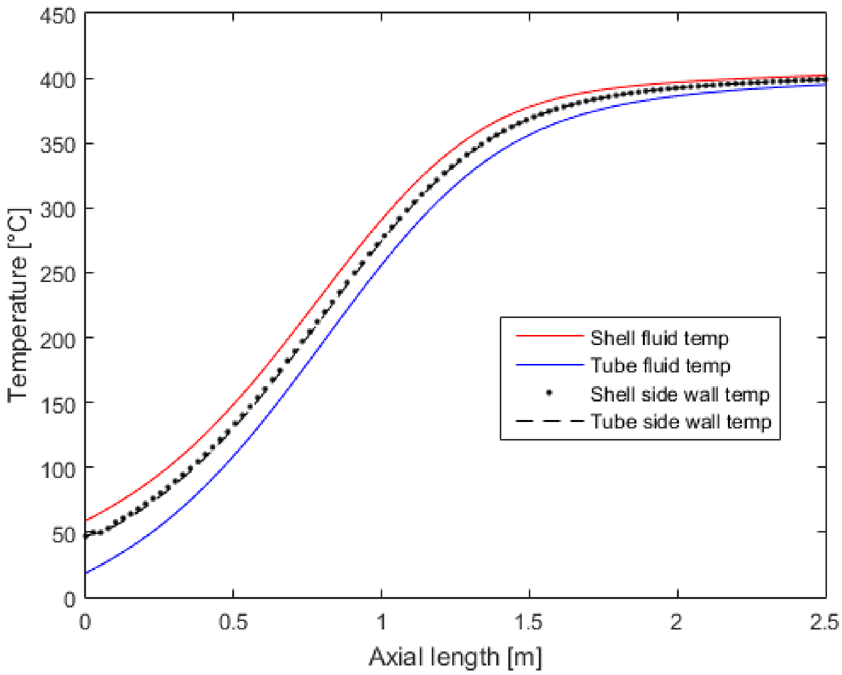

Figure 32: Case E1 hot shell configuration with no heat loss

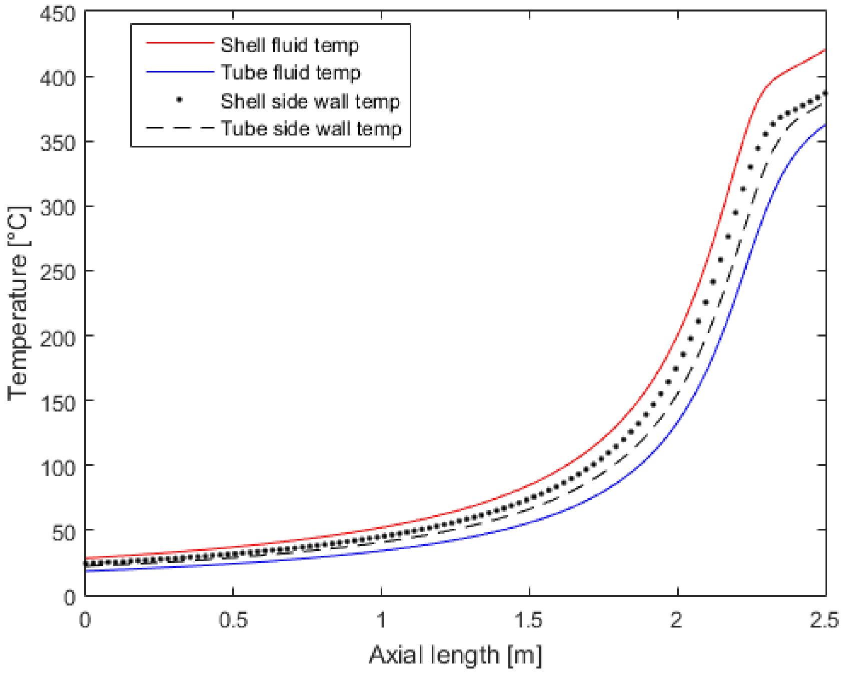

Figure 33: Case F1 hot shell configuration with heat loss

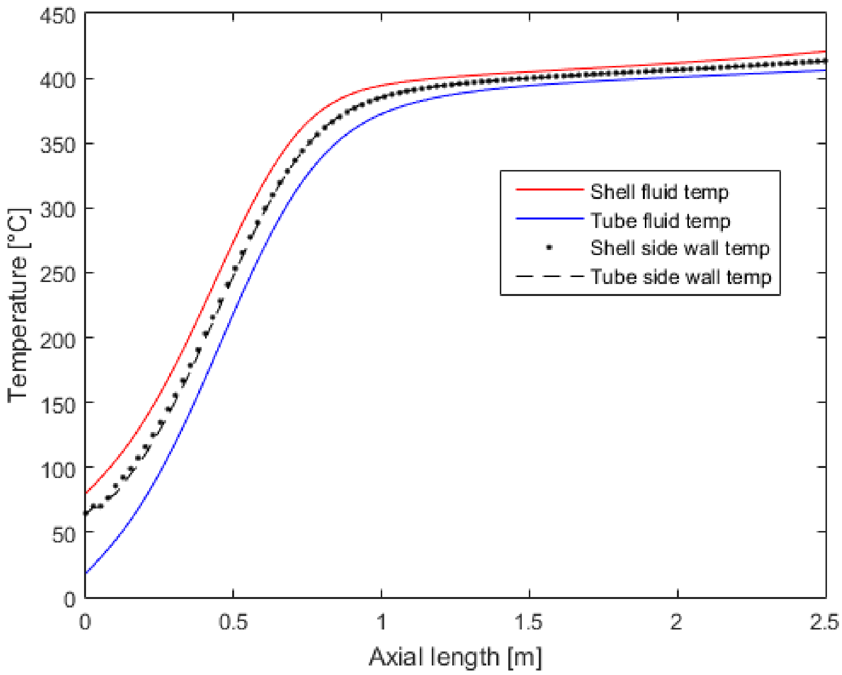

Figure 34: Case F1 hot shell configuration with no heat loss

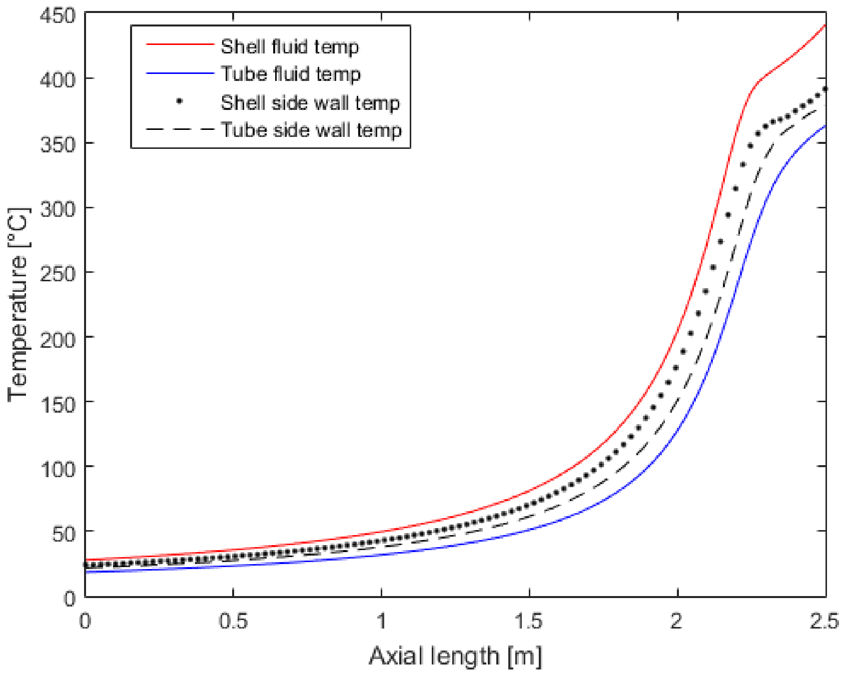

Figure 35: Case G1 hot shell configuration with heat loss

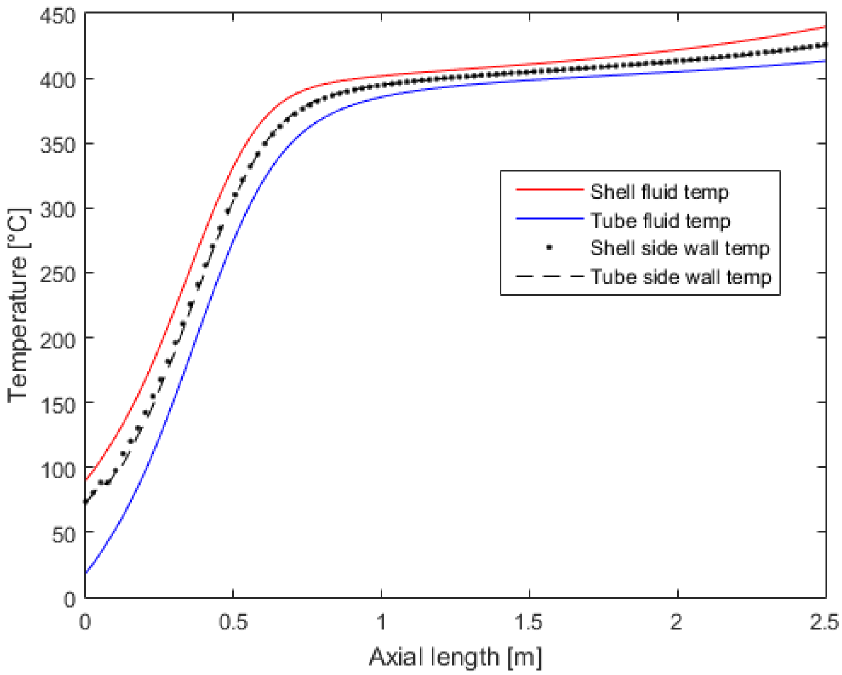

Figure 36: Case G1 hot shell configuration with no heat loss

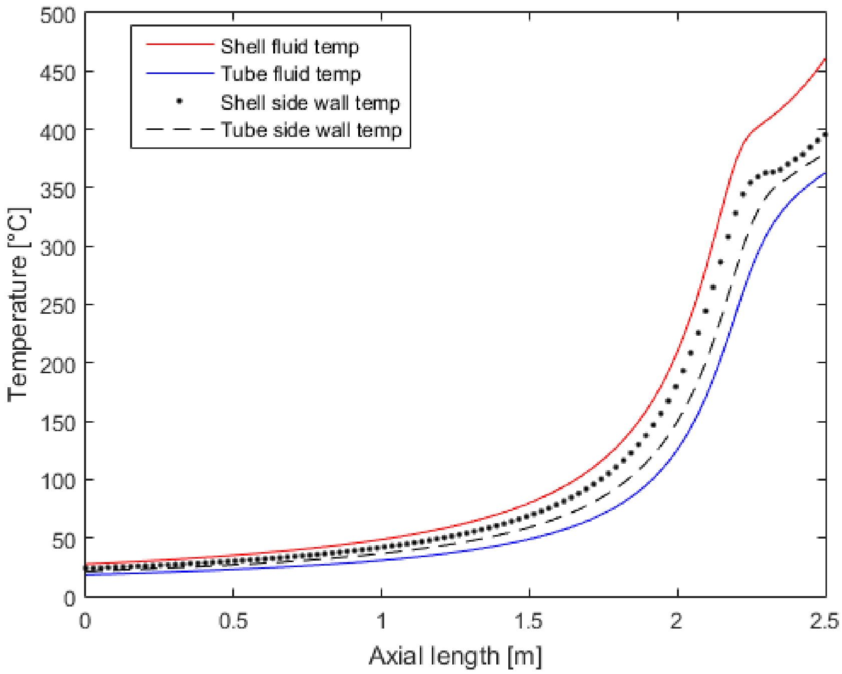

Figure 37: Case H1 hot shell configuration with heat loss

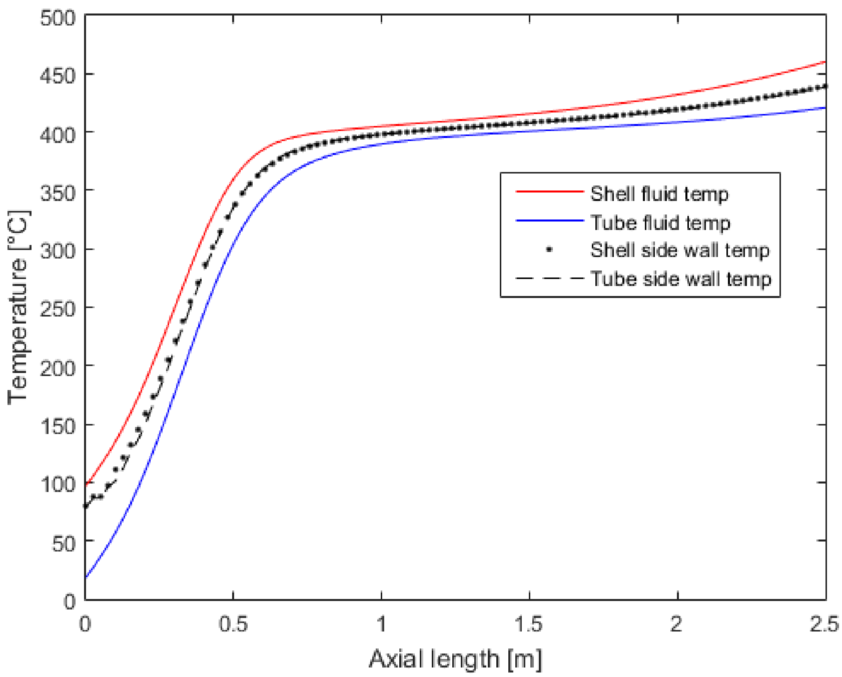

Figure 38: Case H1 hot shell configuration with no heat loss

14 Appendix 3 - Heat exchanger model, hot tube/ cold shell

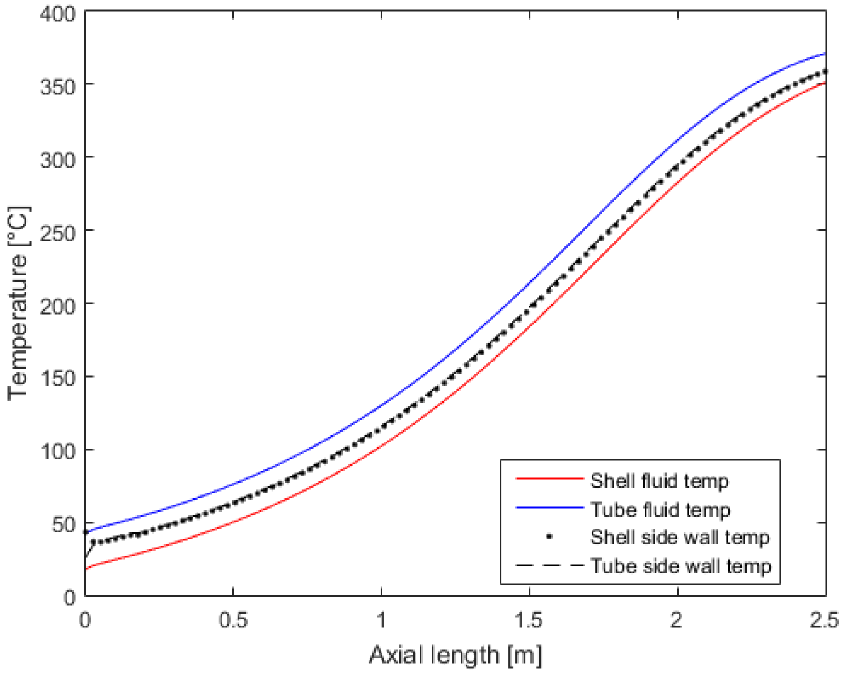

Figure 39: Case A2 hot Tube configuration with heat loss

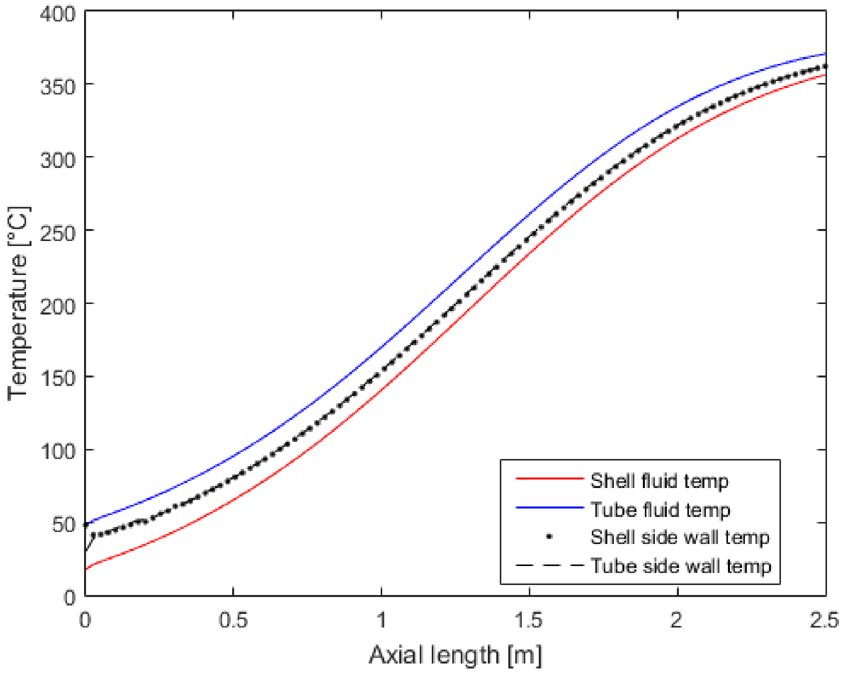

Figure 40: Case A2 hot tube configuration with no heat loss

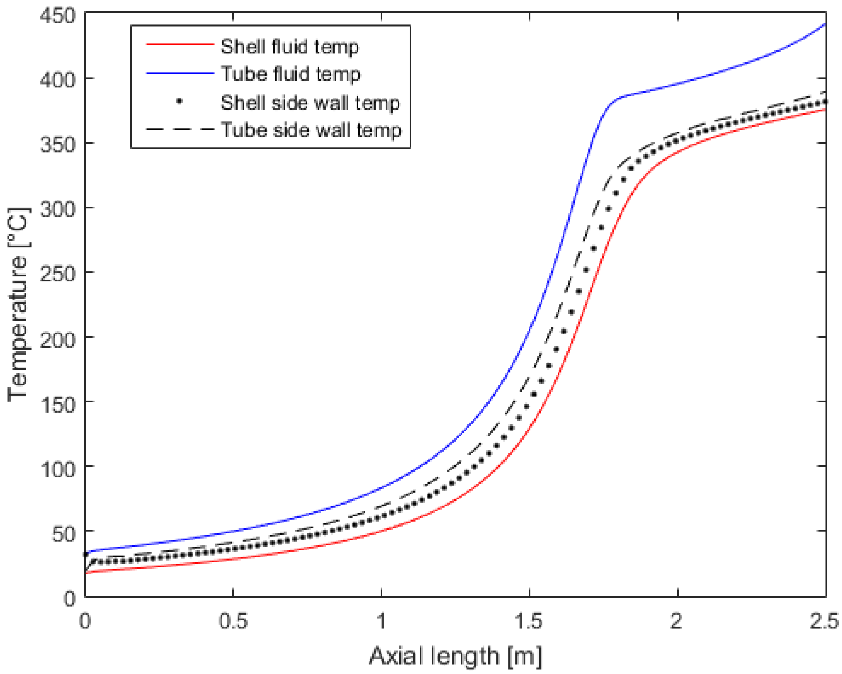

Figure 41: Case B2 hot tube configuration with heat loss

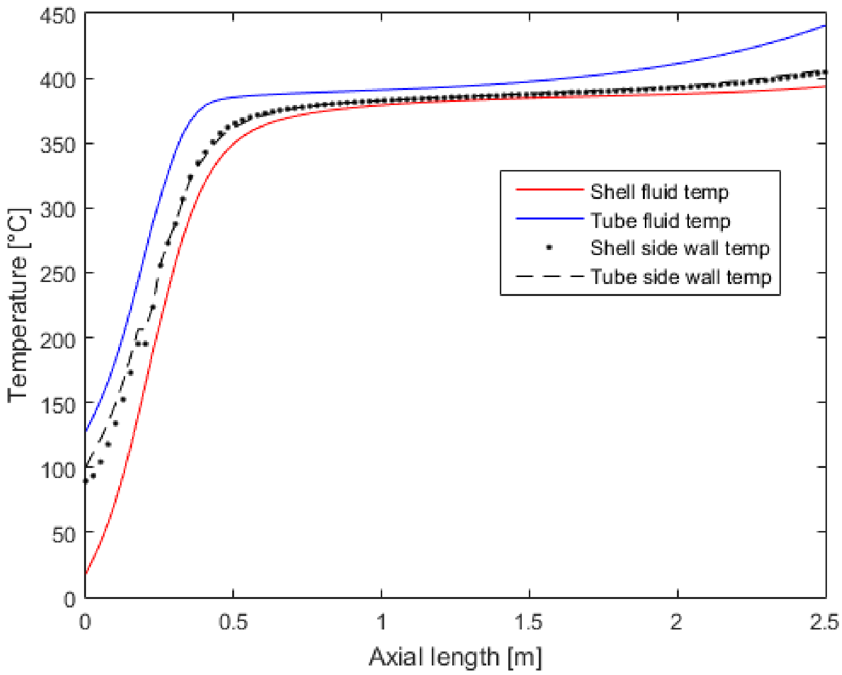

Figure 42: Case B2 hot tube configuration with no heat loss

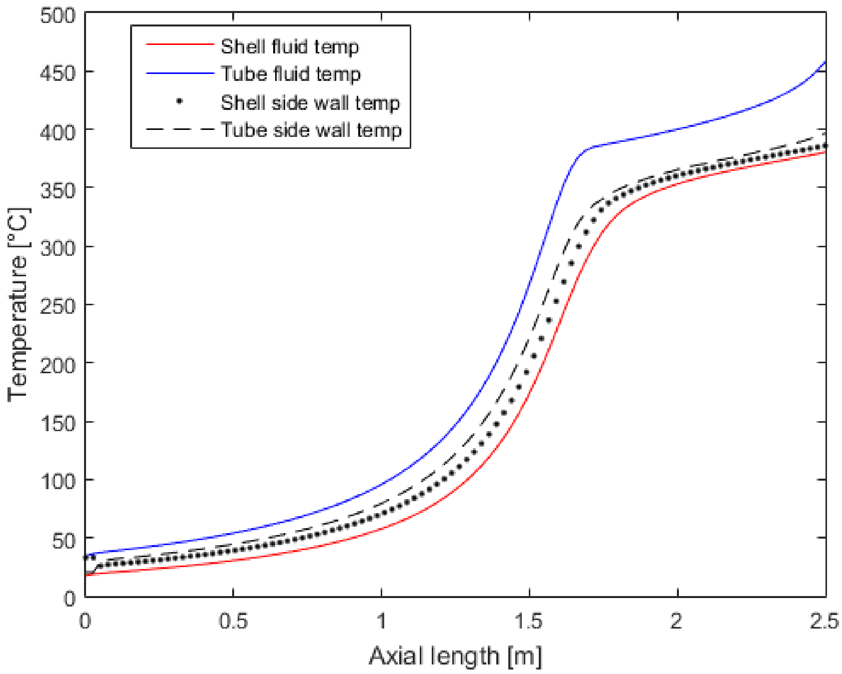

Figure 43: Case C2 hot tube configuration with heat loss

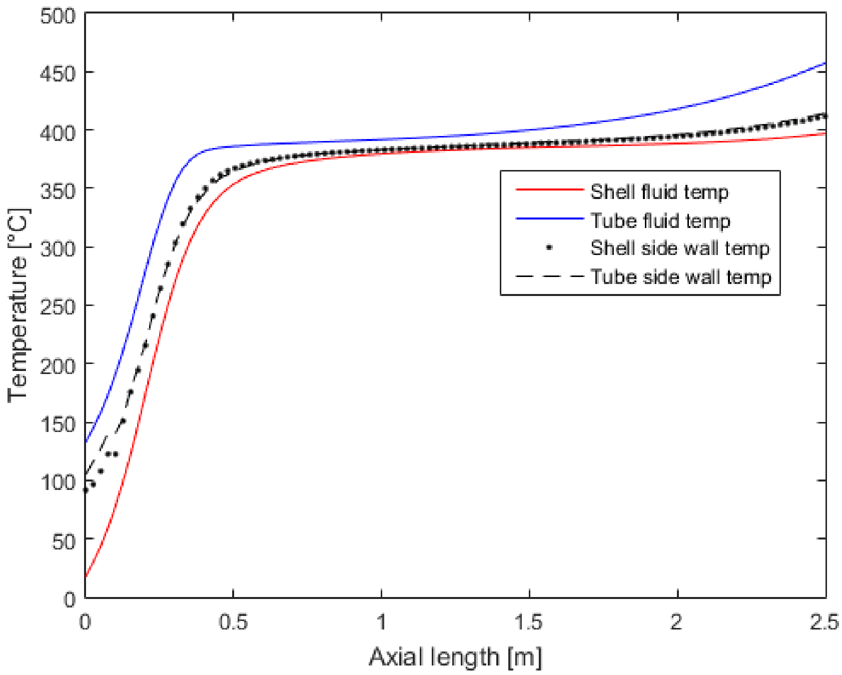

Figure 44: Case C2 hot tube configuration with no heat loss

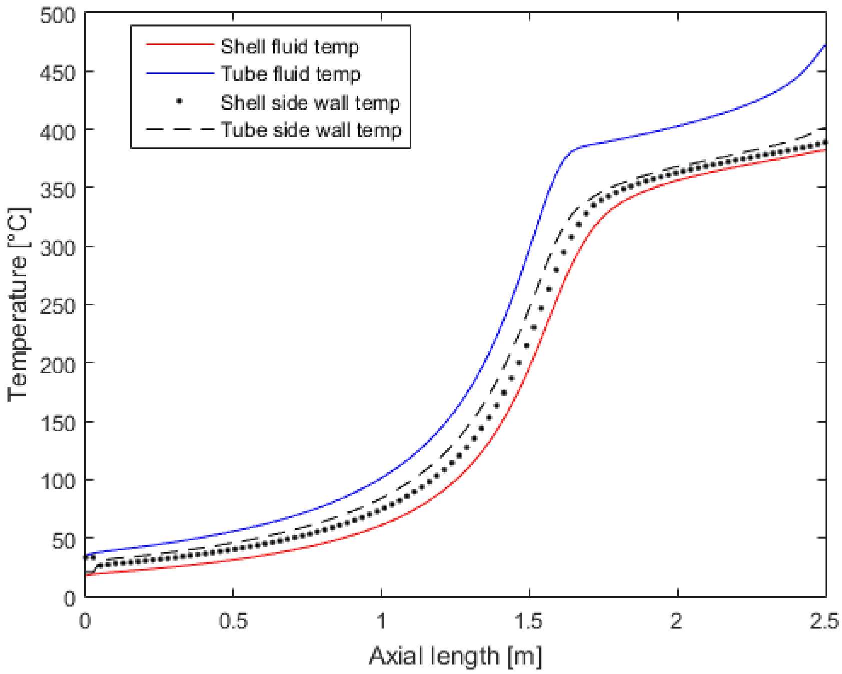

Figure 45: Case D2 hot tube configuration with heat loss

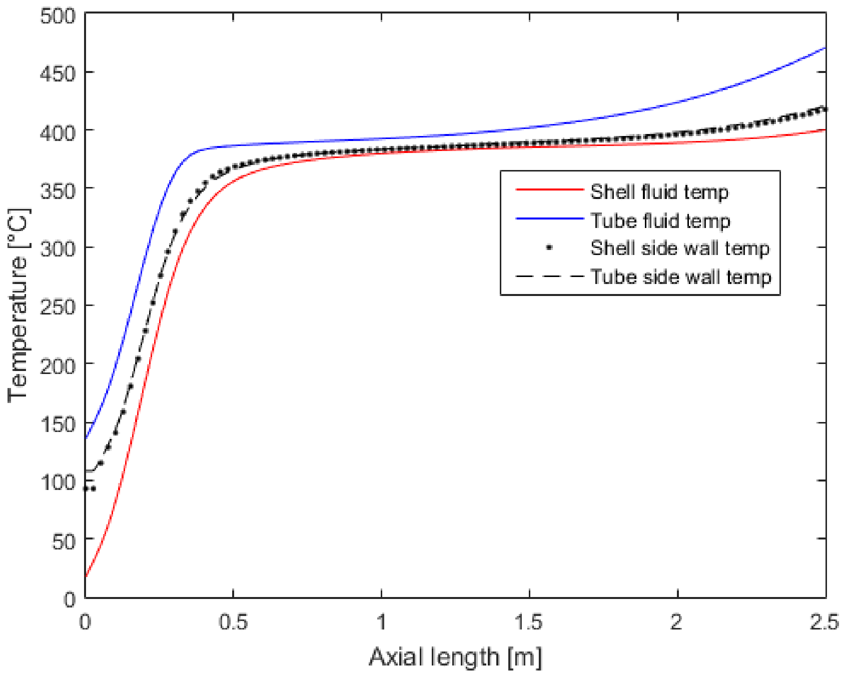

Figure 46: Case D2 hot tube configuration with no heat loss

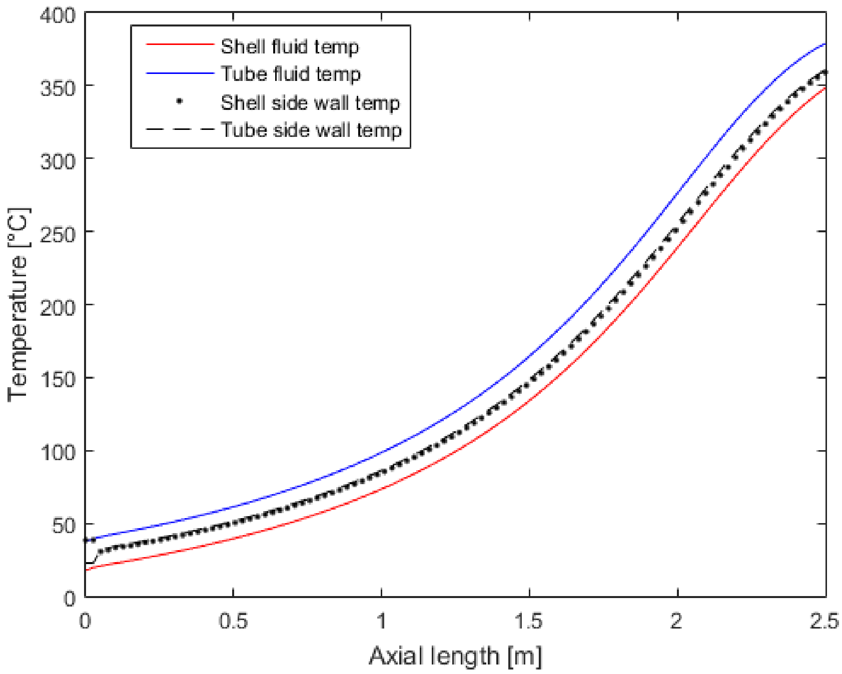

Figure 47: Case E2 hot tube configuration with heat loss

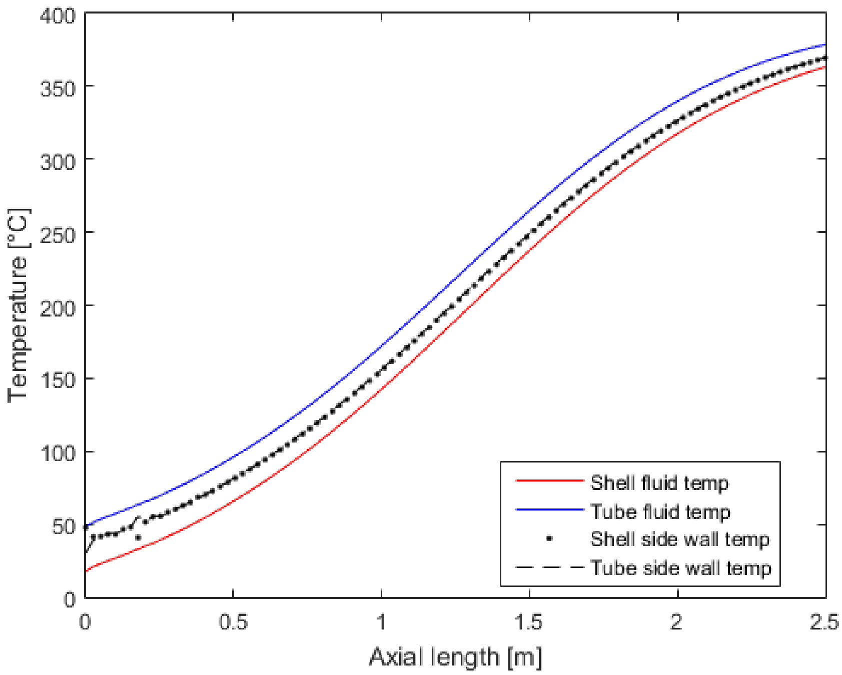

Figure 48: Case E2 hot tube configuration with no heat loss

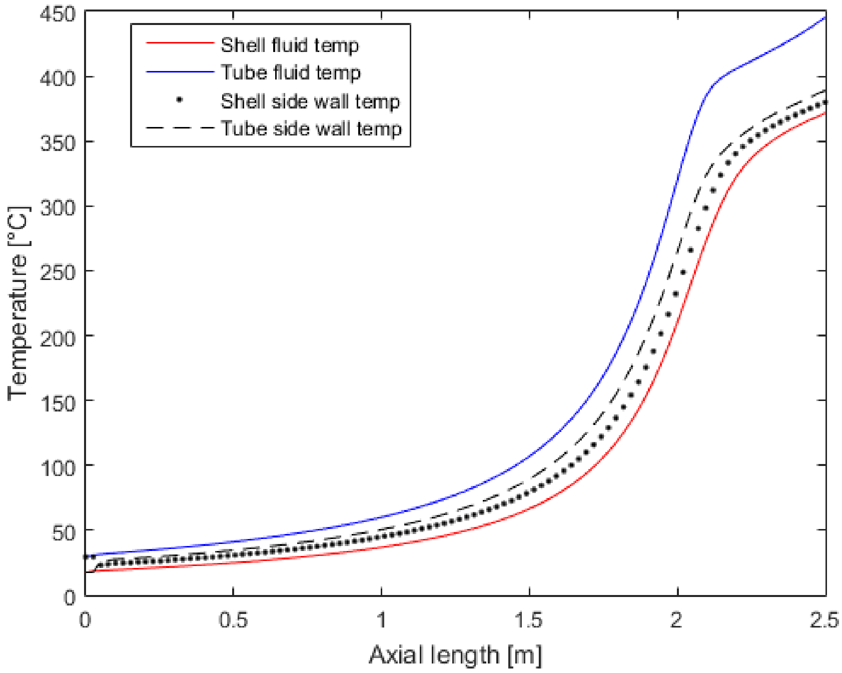

Figure 49: Case F2 hot tube configuration with heat loss

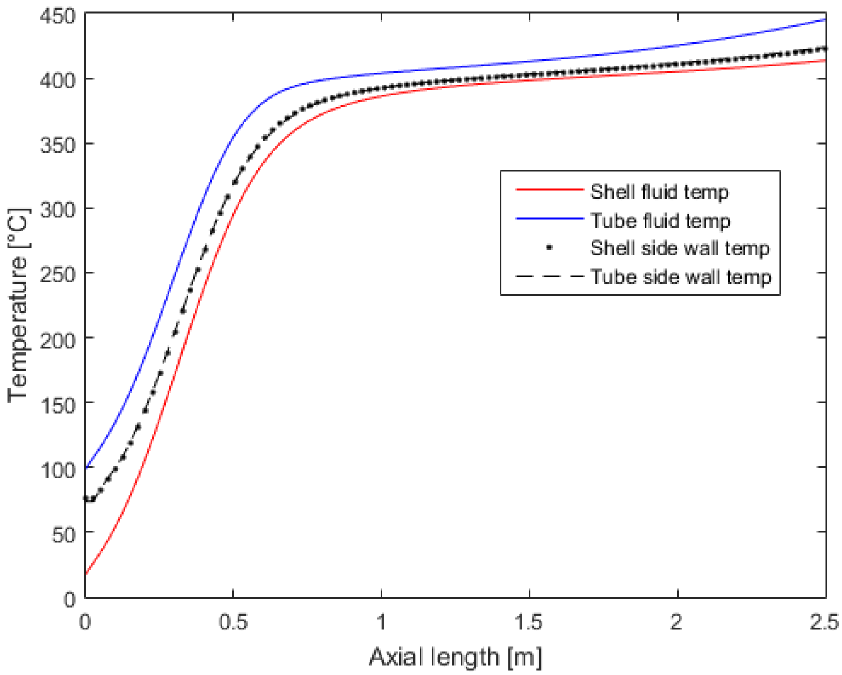

Figure 50: Case F2 hot tube configuration with no heat loss

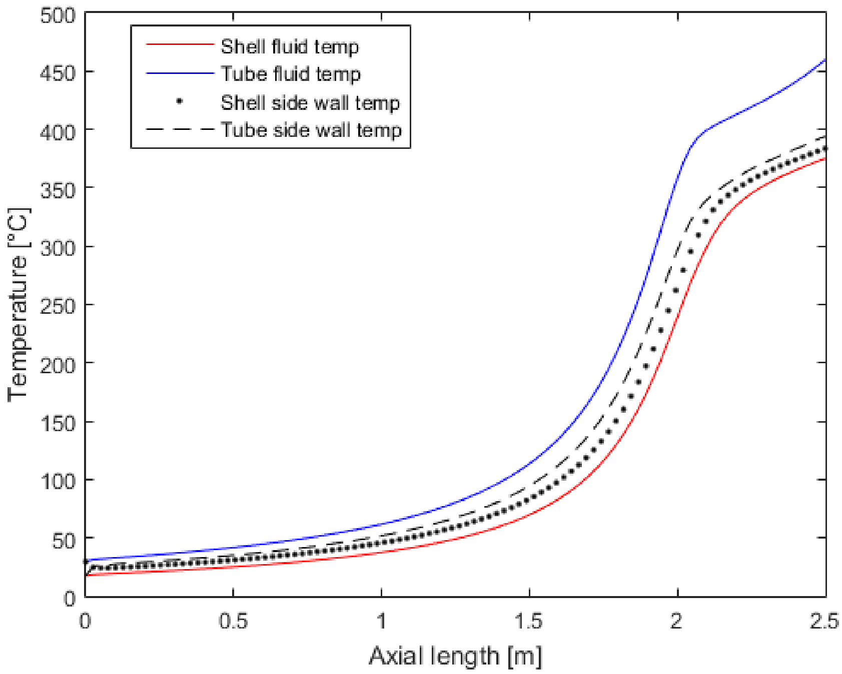

Figure 51: Case G2 hot tube configuration with heat loss

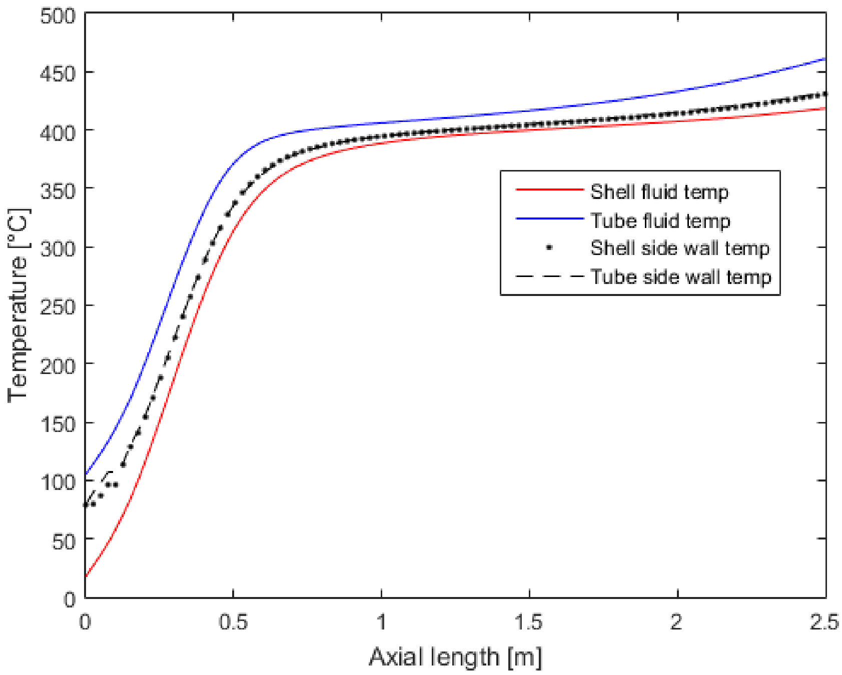

Figure 52: Case G2 hot tube configuration with no heat loss

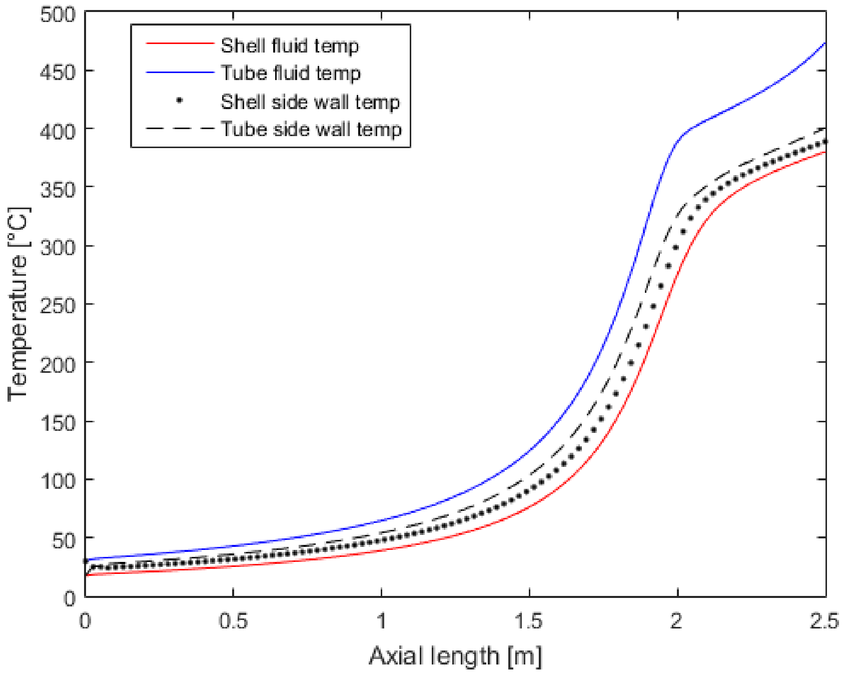

Figure 53: Case H2 hot tube configuration with heat loss

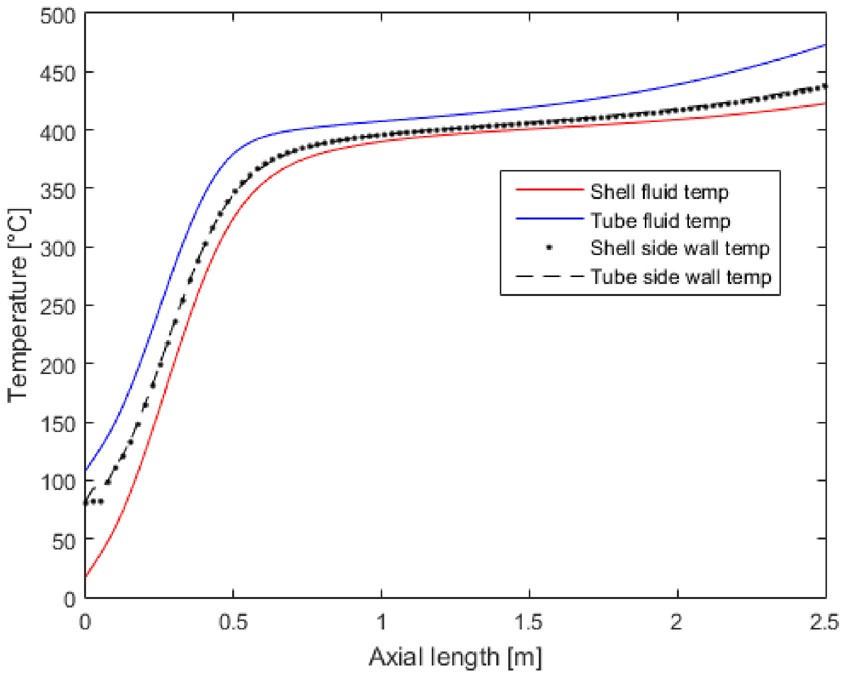

Figure 54: Case H2 hot tube configuration with no heat loss

15 Appendix 4 - Comsol results

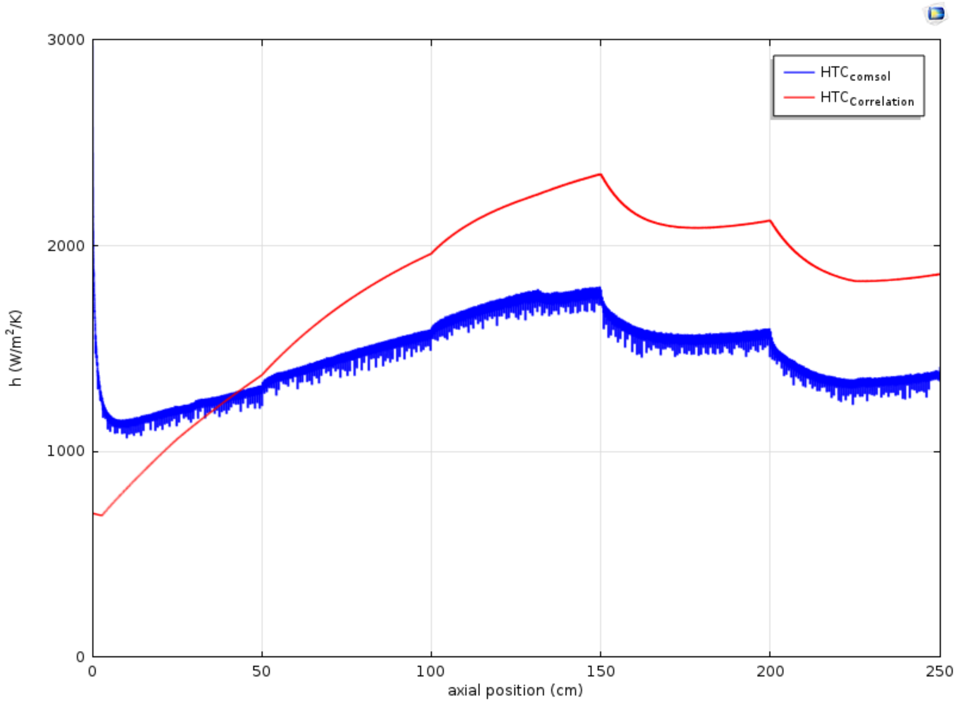

Figure 55: Heat transfer correlation as a function of the axial position at lower temperatures [15], d_t = 3 mm $\phi_m = 1.2 \frac{kg}{hr}$ and p = 300 bar

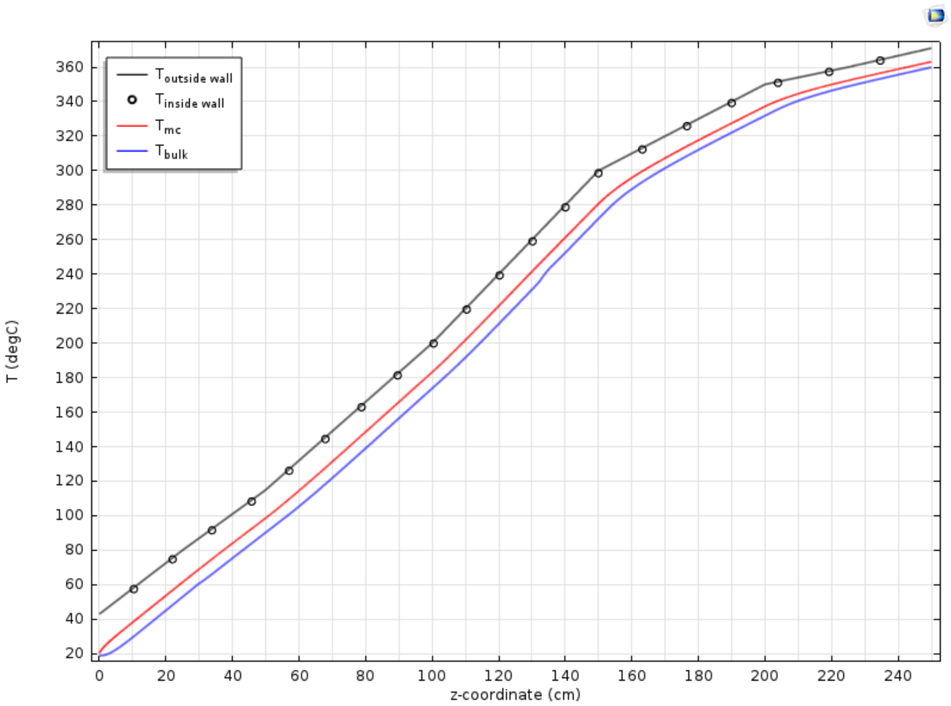

Figure 56: Temperature profile inside the tube for lower temperatures [15], d_t = 3 mm,$\phi_m = 1.2 \frac{kg}{hr}$ and p = 300 bar

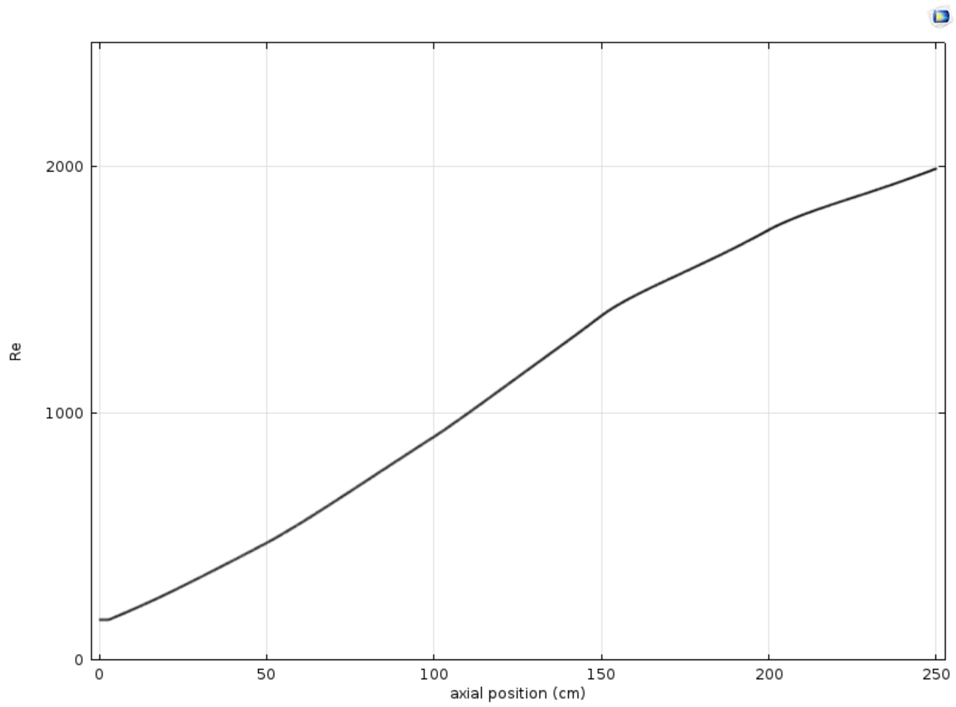

Figure 57: Reynolds number as a function of the axial position for lower temperatures [15], d_t = 3 mm, $\phi_m = 1.2\frac{kg}{hr}$ and p = 300 bar

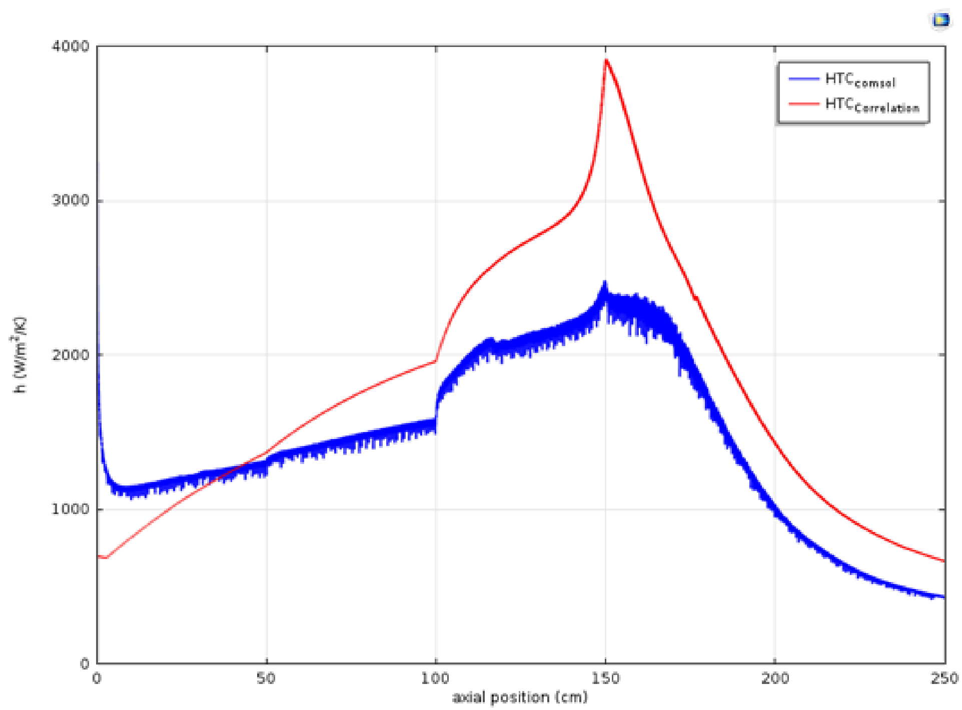

Figure 58: Heat transfer correlation as a function of the axial position at higher temperatures [15], d_t = 3 mm $\phi_m = 1.2\frac{kg}{hr}$ and p = 300 bar

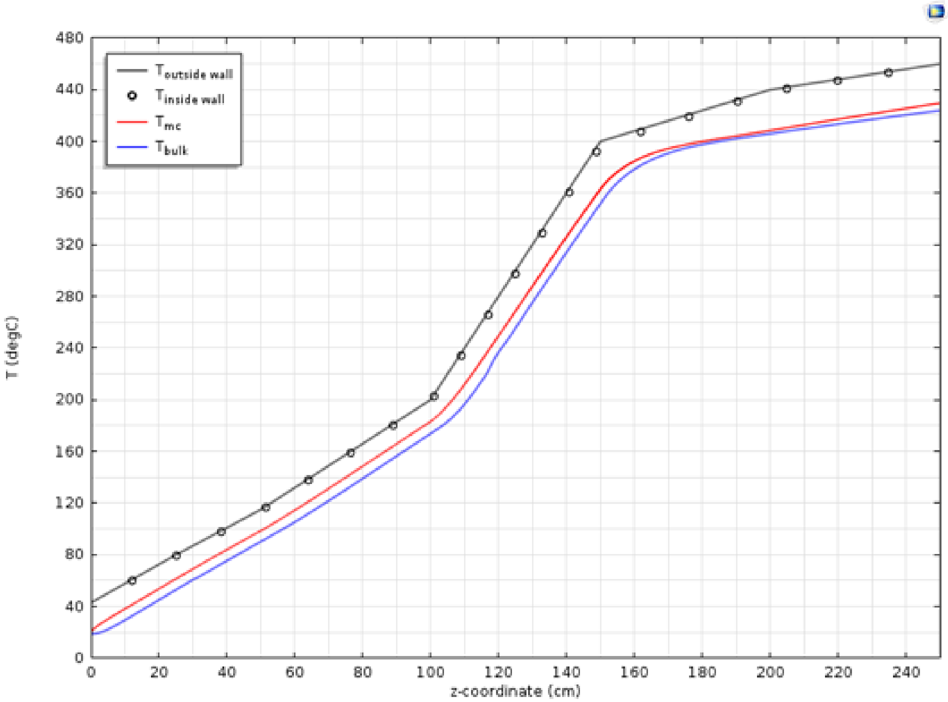

Figure 59: Temperature profile inside the tube for higher temperatures [15], d_t = 3 mm,$\phi_m = 1.2\frac{kg}{hr}$ and p = 300 bar

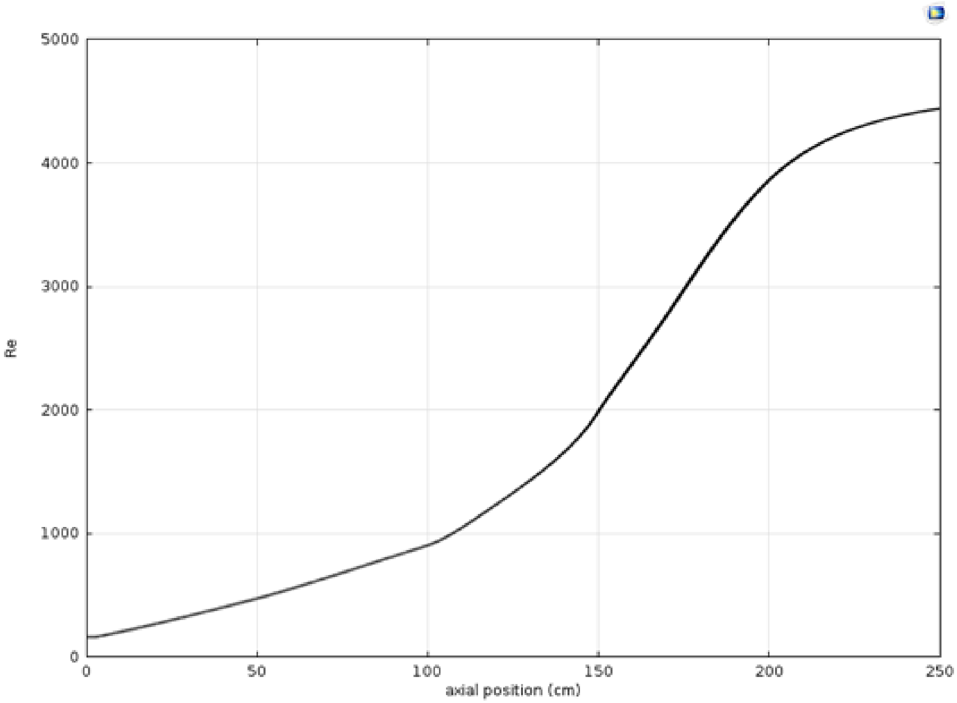

Figure 60: Reynolds number as a function of the axial position for higher temperatures [15], d_t = 3 mm, $\phi_m = 1.2\frac{kg}{hr}$ and p = 300 bar

16 Appendix 5 - Thermal conductivity

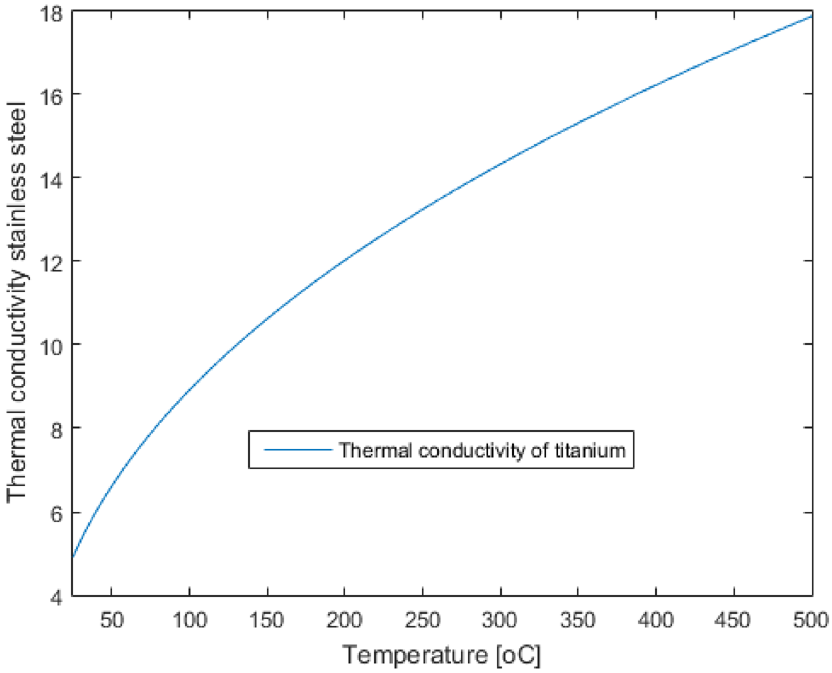

Figure 61: Thermal conductivity of stainless steel. $k = 1.22 * T^{0.432}$. Temperature in Kelvin [15]

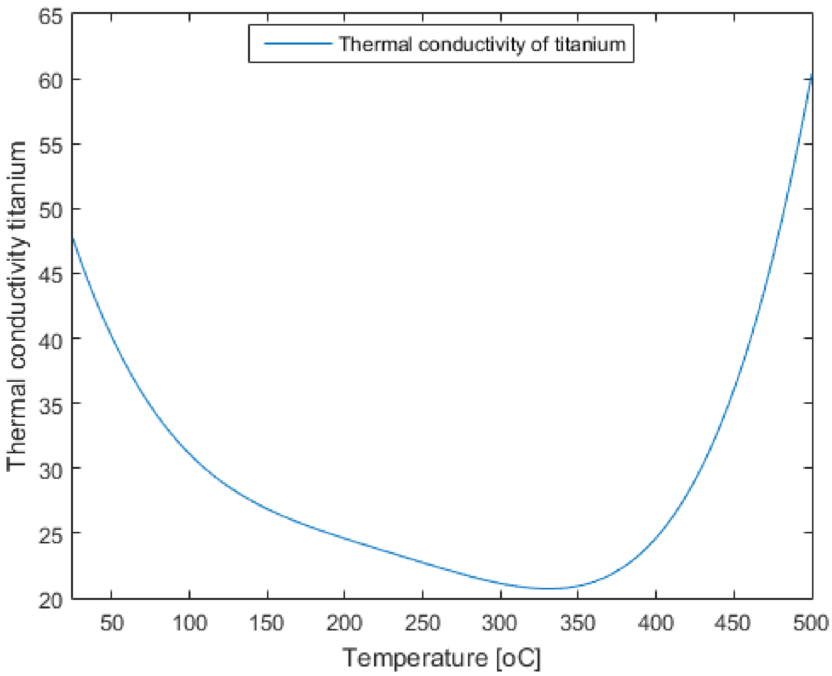

Figure 62: Thermal conductivity of titanium. $k = 58.17412 - 0.4851624 * T + 0.00288092 * T^2 - 8.255595e - 6 * T^3 + 8.903946e - 9 * T^4$ with 50<T<326. $k = 41.95804 - 0.1227486 * T + 2.33331e - 4 * T^2 - 1.937431e - 7 * T^3 + 6.191111e - 11 * T^4$ with 326<T<977. Temperature in Kelvin [15]